Genetic Variation in *Saccharomyces cerevisiae*: Circuit Diversification in a Signal Transduction Network

Brian L. Chin,*,[1] Owen Ryan,[†,‡,§,2] Fran Lewitter,* Charles Boone,[†,‡,§] and Gerald R. Fink*,,[3]**

*Whitehead Institute for Biomedical Research and **Broad Institute of MIT and Harvard, Massachusetts Institute of Technology, Cambridge, Massachusetts 02142, and [†]Banting and Best Department of Medical Research, [‡]Department of Molecular Genetics, and [§]Terrence Donnelly Centre for Cellular and Biomolecular Research, University of Toronto, Toronto, ON M5S 3E1, Canada

ABSTRACT The connection between genotype and phenotype was assessed by determining the adhesion phenotype for the same mutation in two closely related yeast strains, S288c and Sigma, using two identical deletion libraries. Previous studies, all in Sigma, had shown that the adhesion phenotype was controlled by the filamentation mitogen-activated kinase (fMAPK) pathway, which activates a set of transcription factors required for the transcription of the structural gene *FLO11*. Unexpectedly, the fMAPK pathway is not required for *FLO11* transcription in S288c despite the fact that the fMAPK genes are present and active in other pathways. Using transformation and a sensitized reporter, it was possible to isolate *RPI1*, one of the modifiers that permits the bypass of the fMAPK pathway in S288c. *RPI1* encodes a transcription factor with allelic differences between the two strains: The *RPI1* allele from S288c but not the one from Sigma can confer fMAPK pathway-independent transcription of *FLO11*. Biochemical analysis reveals differences in phosphorylation between the alleles. At the nucleotide level the two alleles differ in the number of tandem repeats in the ORF. A comparison of genomes between the two strains shows that many genes differ in size due to variation in repeat length.

RECENT advances in DNA sequencing have identified many nucleotide polymorphisms in the human genome, but it has been challenging to associate this genetic variation to specific phenotypic differences among individuals for complex traits (Jakobsdottir *et al.* 2009; Manolio *et al.* 2009; Dickson *et al.* 2010). This difficulty has been variously attributed to both genetic and nongenetic factors (Hartman *et al.* 2001; Carlborg and Haley 2004; Korbel *et al.* 2007; Dickson *et al.* 2010). Among the genetic factors are many genes contributing a small effect to the final phenotype (QTL) and complex (epistatic) gene interactions. The baker's yeast *Saccharomyces cerevisiae*, with its compact and easily manipulated genome, offers the potential for identifying the relevant polymorphisms and, more importantly, identifying the molecular basis for the phenotypic differences.

Sequence studies comparing *S. cerevisiae* to other yeast species that diverged by 20 million years advanced our understanding of yeast evolution, but did not address how small genetic differences affect phenotypes (Kellis *et al.* 2003). Other studies have examined large numbers of both feral and laboratory *S. cerevisiae* strains, but have focused on population structure and evolutionary origins of the strains rather than the problem of connecting genotype to phenotype (Liti *et al.* 2009; Schacherer *et al.* 2009).

More recently, insights into the genotype-to-phenotype problem have been gained from linkage studies using modern genotyping techniques. Several examples can be seen in the cross of the wild vineyard strain RM11 to the standard laboratory strain S288c. A number of traits have been examined using this cross, including gene expression, cell morphology, resistance to DNA-damaging agents, and telomere length (Brem *et al.* 2002; Gatbonton *et al.* 2006; Nogami *et al.* 2007; Demogines *et al.* 2008). The genetic complexity for most of these traits is high, with many of them influenced by more than three loci. By examining large pools of progeny, recent techniques have

doi: 10.1534/genetics.112.145573
Manuscript received September 4, 2012; accepted for publication October 1, 2012
Available freely online through the author-supported open access option.
Supporting information is available online at http://www.genetics.org/lookup/suppl/doi:10.1534/genetics.112.145573/-/DC1/.
[1]Present address: Department of Systems Biology, Harvard Medical School, Boston, MA, 02115.
[2]Present address: Energy Biosciences Institute, University of California, Berkeley, CA 94720.
[3]Corresponding author: Whitehead Institute/MIT, 9 Cambridge Ctr., Cambridge, MA 02142. E-mail: gfink@wi.mit.edu

further increased the ability to map relevant loci; however, it is still challenging to determine the exact alleles responsible and to understand how those alleles affect the phenotype (Ehrenreich *et al.* 2010; Connelly and Akey 2012).

Recent studies developed a model system that enables a comprehensive assessment of phenotypic differences for the same mutation in the two genetic backgrounds S288c and Σ1278b (Sigma) (Dowell *et al.* 2010). The two strains have very similar genomic sequences: Their divergence of ~0.3% is similar to that between unrelated humans. To assess functional differences between these two strains, ~5100 genes were deleted in Sigma for comparison with the same set of deletions in S288c (Winzeler *et al.* 1999; Dowell *et al.* 2010). The analysis identified strain-specific essential genes. The basis for the strain specificity was likely a complex set of background modifiers.

Here we compare these deletion libraries for the genes that control the key morphogenetic trait of adhesion/filamentation. In Sigma, adhesion requires the filamentation mitogen-activated kinase (fMAPK) pathway, but our library comparison showed that S288c can adhere in the absence of the fMAPK pathway. Although fMAPK-independent adhesion is a complex genetic trait, we devised a transformation protocol that enabled the isolation of *RPI1*, one of the modifiers responsible for the bypass of the fMAPK pathway. *RPI1* is a transcription factor that is polymorphic between S288c and Sigma; the *RPI1* allele from S288c ($RPI1^{S288c}$) confers fMAPK pathway independence by activating *FLO11* transcription, whereas the *RPI1* allele from Sigma ($RPI1^{Sigma}$) cannot. $RPI1^{S288c}$ confers fMAPK pathway independence in either genetic background. Moreover, there is a biochemical difference between the alleles; $RPI1^{S288c}$, but not $RPI1^{Sigma}$ is hyperphosphorylated in both S288c and Sigma. The two forms of *RPI1* differ in the number of tandem repeats in the ORF. A comparison of the S288c and Sigma genomes shows that many other genes with intragenic tandem repeats are highly polymorphic with respect to repeat size, a polymorphism that has been associated with phenotypic changes (Verstrepen *et al.* 2005).

Materials and Methods

Strains, media, microbiological techniques, and growth conditions

Yeast strains used in this study are derived from S288c and Σ1278b. Standard yeast media were prepared and genetic manipulation techniques were carried out as described in Guthrie and Fink (2002). The list of strains used in this study can be found in Supporting Information, Table S5. Adhesion assays were carried out by densely patching strains onto YPD or SC plates. These were grown overnight at 30° and then replica plated onto YPD or SC plates. The replica plates were grown at 30° for 3 days and then washed. The S288c strain expresses *FLO1*, which leads to flocculation that can influence agar adhesion phenotypes. To compare agar adhesion between S288c and Sigma, which does not express *FLO1*, the washes were performed by partially filling the petri dishes with 10 mM EDTA (which disrupts *FLO1*-dependent aggregates) and gentle shaking at ~75 rpm on an orbital shaker. To visualize the difference between the strains, the media used for both the adhesion and the transcription assays were optimized for intrinsic growth differences between S288c and Sigma (*e.g.*, flocculation and mother–daughter cell separation). However, the controls intrinsic to each experiment always permitted a comparison between strains grown under the same media conditions. To induce pseudohyphal growth, single cells were microdissected and grown on SLAD media (Gimeno *et al.* 1992).

The S288c library was constructed using previously published methods (Voynov *et al.* 2006). Each of the 4705 deletion strains in the standard S288c *flo8* library was transformed with a CEN/ARS plasmid carrying the Sigma *FLO8* gene under the control of its own promoter. The 4633 *FLO8* deletion strains successfully recovered from these transformations formed the S288c deletion library. Screening the S288c library and the comparable Sigma deletion library for adhesion uncovered 599 deletions with decreased adhesion (Ahs^-) (Table S1, Table S2, and Table S3). Only 46 deletions affected adhesion the same way in both strains (Table S3).

For quantitative (q)PCR and chromatin immunoprecipitation (ChIP), cells were grown overnight in liquid media as noted, diluted to OD_{600} = 0.25, and grown to OD_{600} = 4–4.5. For protein preparations, cells were grown as for qPCR in synthetic complete media.

Yeast strains carrying gene deletions were constructed by PCR amplification of kanamycin-resistance gene cassettes from the yeast deletion library (Winzeler *et al.* 2000) with ~200 bases of flanking sequence. The list of oligos used in this study can be found in Supporting Information, Table S6. Correct integrants were identified by PCR, with the exception of *tec1Δ*, which was additionally checked by Southern blot using standard techniques (Brown 2001). *FLO11* promoter swaps were carried out by first deleting the *FLO11* promoter with the *URA3* cassette. The reciprocal swap was carried out by PCR amplifying the sequences from each strain and using the PCR products to transform the opposite strain from which the sequence was amplified. The same procedure was performed for the *RPI1* swaps but with only the ORF sequences. 3× FLAG-tagged constructs were created by amplifying the *URA3* cassette from PRS306, using a primer (BCP534) that contained the 3× FLAG epitope. This construct was then subjected to another round of PCR to add 50 bp of flanking homology to the *RPI1* C terminus. The resulting PCR product was used for transformation. The haploid *MAT***a** deletion collection was transformed with plasmid pHL1, using previously published protocols (Liu *et al.* 1996; Voynov *et al.* 2006).

GFP measurements

Cultures for GFP measurements were grown overnight in liquid YPD in 96-well plates and then pelleted and resuspended

in water. Samples were transferred to Corning 96-well black clear-bottom plates and OD_{600} and GFP fluorescence were measured in a Tecan Safire2 plate reader. For backcrosses, high-fluorescing progeny were backcrossed to the low-fluorescing Sigma *tec1Δ* for three generations.

tec1Δ bypass screen

The *CLN2* PEST sequence was added to the end of the *HIS3* gene to target the protein product to the proteasome. Without this modification, a Sigma *FLO11pr-HIS3*, *tec1*Δ strain produces enough His3p protein from the *FLO11* promoter to be His^+, even in relatively high concentrations of the His3p competitive inhibitor 3-aminotriazole. The *HIS3-PEST* construct was created by Infusion PCR cloning (Clontech) the PEST sequence from *CLN2* immediately upstream of the *HIS3* stop codon in PRS315. The *CLN2* PEST sequence was amplified using primers BCP316 and BCP317 and PRS315 was linearized by PCR using primers BCP320 and BCP321. To create the *FLO11pr-HIS3-PEST* strain, the *HIS3-PEST* construct was PCR amplified with primers BCP249 and BCP324. These primers have homology to replace the endogenous *FLO11* ORF with the *HIS3-PEST* ORF, and the PCR product was transformed into yBC172. Transformants were selected on −HIS media and then correct transformants were screened for by PCR. *TEC1* was deleted in *FLO11pr-HIS3-PEST* transformants by PCR transformation.

The *FLO11pr-HIS3-PEST*, *tec1Δ* strain was transformed with an S288c CEN/ARS genomic library (Rose *et al.* 1987). Transformants were first selected for 24 hr on −URA plates and then replica plated onto −URA, −HIS plates plus 5 mM 3-amino-1,2,4-triazole.

We obtained ∼300 His^+ transformants from >15,000 total transformants, and we examined whether the His^+ phenotype was dependent upon the plasmid by selecting for strains that had lost the plasmid on 5-FOA. After 5-FOA selection, these strains were examined, by dilution series, on −HIS plates.

Fifty-four strains required the library plasmid to be His^+, and the plasmid from these strains was isolated and the ends of the insert were sequenced. Potential bypass strains were identified by examining the overlapping regions among the inserts.

qPCR

Total RNA was obtained by standard acid phenol extraction from 2 ml of culture. The QIAGEN (Valencia, CA) QuantiTect Reverse Transcription Kit was used to remove residual genomic DNA and reverse transcribe the RNA templates to generate cDNAs. Aliquots of cDNA were used in real-time PCR analyses with reagent from Applied Biosystems (Foster City, CA) and the ABI7500 real-time PCR system.

Chromatin IP

Protocols have been described in Lee *et al.* (2006). Briefly, IPs were performed with Dynal Protein G magnetic beads preincubated with antibodies against FLAG epitope (Sigma M2). To examine enrichment, SYBR Green qPCR (Applied Biosystems) was performed on IP and whole cell extract, using gene-specific primers.

Protein manipulations

Total protein was extracted using standard TCA precipitation with slight modifications (Graham 2001). Namely, after TCA precipitation the acetone wash was omitted and instead the cells were washed once with 1 M Tris, pH 8. For phosphatase assays, 5 μl of total protein was treated with 2 μl λ-phosphatase (New England Biolabs, Beverly, MA) for 2 hr at 30° and the reaction was stopped by adding 6× Laemmli loading buffer to 1× concentration and boiling for 10 min. Samples were run out on a 10% TGX gel [Bio-Rad (Hercules, CA) 456-1036S]. The phosphorylation of *RPI1* causes it to run as a diffuse smear and the amount of signal is distributed across this entire range. To visualize phosphorylated *RPI1* alongside phosphatase-treated *RPI1*, up to five times the amount of phosphorylated *RPI1* was loaded. Blotting against FLAG was performed using HRP-conjugated anti-FLAG M2 antibody (Sigma A8592).

Bioinformatics

Gene ontology term enrichment was performed using the AMIGO term enrichment tool version 1.8 (http://amigo.geneontology.org/cgi-bin/amigo/term_enrichment).

To find intragenic repeats, the EMBOSS program ETANDEM (Rice *et al.* 2000) was used to screen the sequences of all *S. cerevisiae* (S288c version 2010 downloaded from the *Saccharomyces* Genome Database in April 2011) and the ∑1278b strain (Sigma downloaded from http://mcdb.colorado.edu/labs1/dowelllab/pubs/DowellRyan/ in October 2010) for repeat units of length 3–500 bp. For each ORF, we compared the length in the two strains. We screened 6685 ORFs in S288c and 6450 ORFs in Sigma. A total of 6439 ORFs were common to both strains. Of these 6439 ORFs, 5928 were identical in length. Of the remaining 511 ORFs, 127 ORFs differed in total length by at least 6 bp and showed a length difference in the repeat region of at least 6 bp. We eliminated an additional 11 ORFs because of large truncations in either the 5′ or the 3′ region of the ORF, accounting for the length differences between strains. All but 9 of the length differences in the 116 ORFs were a multiple of 3. These discrepancies could be due to sequencing errors. The length of the ORF was longer in Sigma for 60 ORFs (43 ORFs with base pair differences of 6–33, and 17 ORFs with base pair differences of ≥36). A total of 56 ORFs were longer in S288c (43 ORFS with base pair differences of 6–33, and 13 ORFs with base pair differences of ≥36).

Repeat length PCRs

Primers flanking the repeat region were designed using PRIMER3 (Rozen and Skaletsky 2000). PCR products were visualized on 10% polyacrylamide gels.

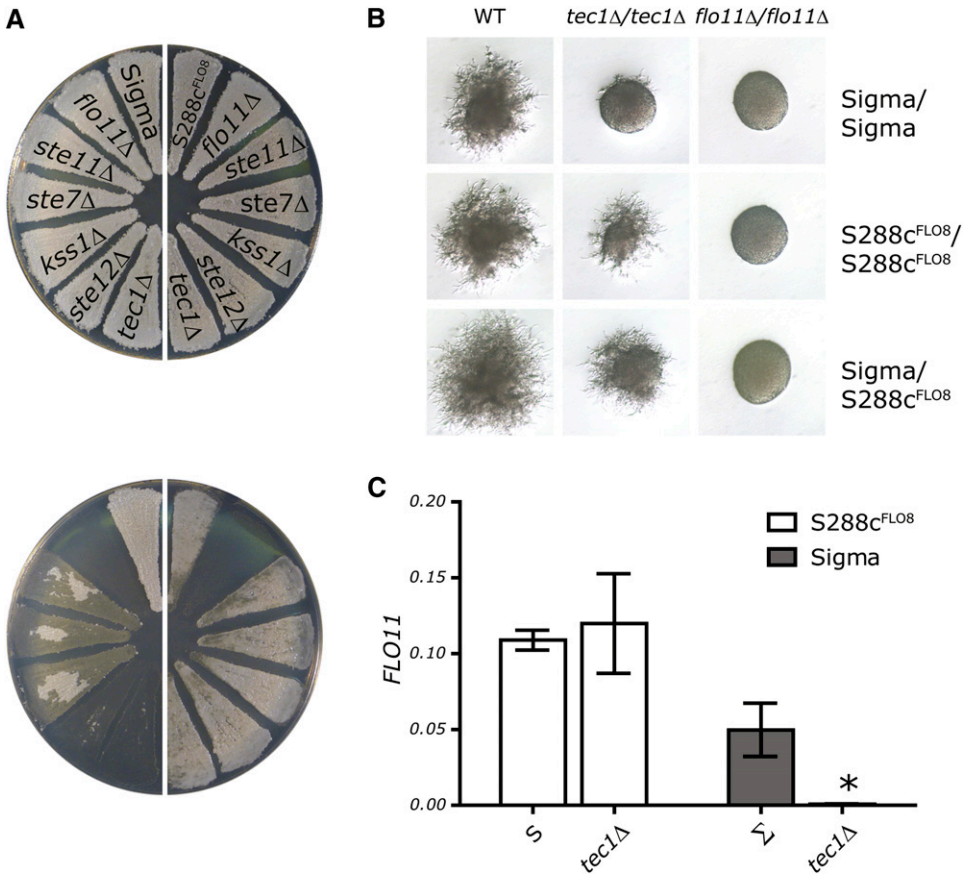

Figure 1 The fMAPK pathway is not required for *FLO11* expression in S288c. (A) Adhesion assays performed on S288c strains (right half of the plate) or Sigma strains (left half of the plate). The same plate is shown before (top) and after (bottom) washing. (B) Pseudohyphal growth on SLAD media for diploid Sigma, S288c, or Sigma/S288c hybrids. (C) qPCR assay of *FLO11* transcript levels was performed on Sigma and S288c strains that were WT or *tec1Δ*. Mean *FLO11* levels normalized to *ACT1* levels are presented ± SD. $*P < 0.01$ compared to WT.

Results

Creation of an S288c FLO8 deletion library

Systematic deletion library comparison of S288c and Sigma for the adhesion phenotype required the creation of a new S288c *FLO8* library because the progenitor to the standard S288c deletion library carries a *flo8* mutation that prevents adhesion to agar. When S288c *flo8* is transformed to Flo8$^+$, it adheres in a *FLO11*-dependent fashion (Liu *et al.* 1996). We next assayed the entire library for the adhesion phenotype (Adh$^+$ or Adh$^-$) and identified deletions in the S288c library with the Adh$^-$ phenotype.

The fMAPK pathway is required for adhesion and FLO11 transcription in Sigma but not in S288c

Comparison of the loss of adhesion mutants in the Sigma and S288c deletion libraries revealed that many genes have strain-specific roles in adhesion (Table S1, Table S2, and Table S3). The strain specificity of the Ahs$^-$ phenotypes is not attributable to an integrated *FLO8* in the Sigma library, but to a plasmid-borne *FLO8* in the S288c library. The Ahs$^-$ phenotype was the same in 28/30 deletions tested from the S288c deletion library whether *FLO8* was plasmid borne or integrated at the resident *FLO8* locus (replacing the *flo8* allele). All strains pursued further had the *FLO8* gene integrated at its native locus in S288c.

The comparison of S288c and Sigma adhesion mutants revealed that the fMAPK pathway is required for adhesion in Sigma but it is not required for adhesion in S288c (Figure 1A). Strains carrying deletions in kinase genes—*STE7*, *STE11*, and *KSS1*—and the transcription factor genes—*STE12* and *TEC1*—have a clear adhesion defect in Sigma but adhere well in S288c (Figure 1A). qPCR measurements revealed that wild-type S288c and S288c *tec1Δ* both show strong expression of *FLO11*, whereas Sigma *tec1Δ* has a 50-fold decrease in *FLO11* RNA levels relative to the wild-type control (Figure 1C). The distinct requirement for the fMAPK pathway in Sigma but not in S288c suggests that adhesion is controlled differently in the two strains.

The fMAPk pathway in Sigma activates *FLO11* transcription for haploid adhesion and diploid filamentation (Liu *et al.* 1993; Roberts and Fink 1994; Lo and Dranginis 1998). To determine whether the fMAPK pathway is dispensable for diploid filamentation in S288c, we constructed diploid S288c strains. Filamentation in the S288c *tec1Δ*/*tec1Δ* strain is indistinguishable from that in wild type, whereas the Sigma *tec1Δ*/*tec1Δ* strain has a filamentation defect (Figure 1B). A hybrid S288c/Sigma *tec1Δ*/*tec1Δ* strain is able to filament, showing that the ability of S288c to bypass an fMAPK defect for filamentation is dominant. Homozygous diploid S288c *flo11Δ*/*flo11Δ* and Sigma *flo11Δ*/*flo11Δ* strains failed to form filaments. Thus, *FLO11* function is required for adherence and filamentation

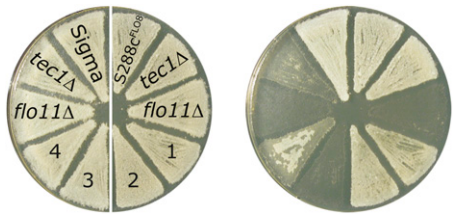

Figure 2 S288c with *FLO11pr*^{Sigma}::*FLO11* is fMAPK independent. Agar adhesion assays were performed on S288c strains (right half of the plate) or Sigma strains (left half of the plate) in the *FLO11* promoter swap experiment (see text). The same plate is shown before (left) and after (right) washing. Strains with their endogenous *FLO11* promoter are labeled with their relevant genotype. Strains carrying a swapped *FLO11* promoter are labeled numerically: (1) S288c *FLO11pr*^{Sigma}::*FLO11*; (2) S288c *FLO11pr*^{Sigma}::*FLO11*, *tec1Δ*; (3) Sigma *FLO11pr*^{S288c}::*FLO11*, *tec1Δ*; and (4) Sigma *FLO11pr*^{S288c}::*FLO11*.

in both S288c and Sigma even though the requirement for the fMAPK pathway is restricted to Sigma.

Differences in the FLO11 promoter sequence do not account for S288c fMAPK-independent FLO11 expression

Reciprocal promoter swap strains were used to determine whether the sequence differences between the S288c and Sigma *FLO11* promoters (*FLO11pr*^{S288c} and *FLO11pr*^{Sigma}, respectively) could account for the fMAPK independence of S288c. S288c *FLO11pr*^{Sigma} adhered like a wild-type S288c as did S288c *FLO11pr*^{Sigma} *tec1Δ*, showing that *FLO11pr*^{S288c} is not necessary for fMAPK-independent adhesion of S288c cells (Figure 2). *FLO11* RNA levels in the S288c *FLO11pr*^{Sigma} strain were consistent with the adhesion phenotypes; specifically, in S288c there was no significant difference in *FLO11* RNA levels, regardless of the promoter or the presence of a *tec1*Δ (Figure S1A).

The *FLO11pr*^{S288c} does not promote *FLO11* transcription as efficiently in Sigma as it does in S288c. This difference is reflected both in the adhesion assay and in the qPCR measurement of *FLO11* RNA levels (Figure 2 and Figure S1B). Nevertheless, the *FLO11pr*^{S288c} in Sigma is *TEC1* dependent for both adhesion and *FLO11* transcription, whereas it is *TEC1* independent in S288c. These results imply that the sequence differences in the promoters are not responsible for the fMAPK independence of S288c.

The strain difference in FLO11 regulation is genetically complex

Crosses between the adherent S288c *tec1Δ* strain and the nonadherent Sigma *tec1Δ* strain did not yield a simple segregation pattern for adherence:nonadherence. Analysis of 24 complete meiotic tetrads produced novel phenotypes (24/96 progeny were clearly adherent, 56/96 were nonadherent, and 16/96 displayed various partially adherent phenotypes) (Figure S2). Backcrosses of the F_1 adherent progeny to the Sigma *tec1Δ* strain continued to yield non-Mendelian segregations and novel adherent phenotypes.

We considered the possibility that the failure to isolate modifiers by backcrosses was due to the lack of robustness of the adhesion assay. Moreover, agar adhesion can be affected by both transcriptional and posttranscriptional regulation of *FLO11* (Voynov *et al.* 2006; Wolf *et al.* 2010). In addition, *FLO11* manifests epigenetic switching between on and off states (Halme *et al.* 2004; Bumgarner *et al.* 2009). To quantitatively assess the *FLO11* phenotype we used a *FLO11pr*::*GFP* construct to monitor the segregation of *FLO11* transcription in S288c *tec1*Δ × Sigma *tec1*Δ crosses. These crosses directly examined the variation affecting *FLO11* transcription, yet the segregation of GFP fluorescence was still complex in both the F_1 generation and subsequent backcrosses (Figure S3).

Tetrad analysis of crosses between the adherent wild-type S288c and Sigma strains provided further insight into the cause of the anomalous segregation patterns. Since both wild-type strains were adherent, we expected the F_1 progeny would all be adherent. However, many of the F_1 progeny were nonadherent (Figure S4). These data suggest that polymorphisms between wild-type Sigma and S288c combine in the progeny to suppress *FLO11* expression. This situation considerably complicates using either conventional tetrad genetic analysis or bulk segregation analysis to find alleles that bypass the fMAPK pathway. Isolation and analysis of any of the many polymorphisms contributing to fMAPK independence required another approach.

Transformation permits the isolation of a modifier from S288c conferring fMAPK-independent expression of FLO11

To overcome the challenges of mapping polymorphisms for fMAPK-independent adhesion, we developed a transformation protocol to select for plasmids carrying S288c genes that bypass the fMAPK pathway. The selection required replacement of the *FLO11* ORF with a *HIS3-PEST* construct in the Sigma *tec1*Δ strain. This PEST modification enabled the visualization of slight differences in *FLO11* expression when selecting for His$^+$ transformants. The Sigma *FLO11pr-HIS3-PEST*, *tec1*Δ strain is His$^-$ whereas the S288c *FLO11pr-HIS3-PEST*, *tec1*Δ strain is His$^+$. Modifiers from S288c that could bypass the requirement for the fMAPK pathway in Sigma were obtained by transforming the Sigma *FLO11pr-HIS3-PEST*, *tec1*Δ strain (His$^-$) with a S288c CEN/ARS genomic library (Rose *et al.* 1987) and selecting for His$^+$ transformants.

Sequence analysis of the plasmids capable of conferring the His$^+$ phenotype to the Sigma *FLO11pr-HIS3-PEST*, *tec1*Δ strain identified several genes (including *TEC1* itself). A gene with a relevant S288c polymorphism should have a sequence difference from its Sigma allele and the ability to confer the His$^+$ phenotype (bypass the *tec1*Δ defect) when integrated in the chromosome in a single copy. *RPI1*^{S288c} was the only gene obtained that fulfilled these criteria. When *RPI1*^{S288c} replaced *RPI1*^{Sigma} in the chromosome, the Sigma *FLO11pr-HIS3-PEST*, *tec1*Δ strain was His$^+$. Moreover,

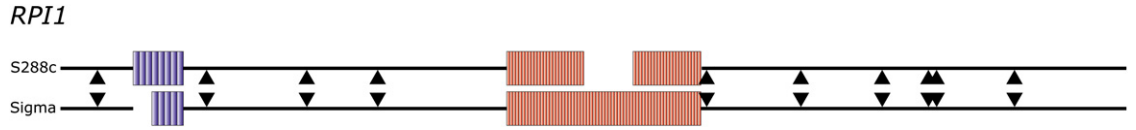

Figure 3 *RPI1* alleles vary in the number of intragenic repeats. The S288c and Sigma alleles of *RPI1* have intragenic repeats, but the repeat lengths differ between the two strains. The schematic illustrates the alignment of the two alleles. The boxes represent individual repeat elements and arrowheads represent locations of SNPs. Open areas represent the shortened repeat length in that allele.

$RPI1^{S288c}$ and $RPI1^{Sigma}$ differ in numerous SNPs and stretches of intragenic repeats that differ in length (Figure 3, Figure S5, and Figure S6).

$RPI1^{S288c}$ but not $RPI1^{Sigma}$ is a bypass suppressor of the fMAPK pathway

Consistent with the hypothesis that $RPI1^{S288c}$ has an allele-specific role in *FLO11* expression, deletion of $RPI1^{S288c}$ in S288c results in a strong adhesion defect and decreased *FLO11* RNA, whereas deletion of $RPI1^{Sigma}$ in Sigma does not (Figure 4, A–C). To further characterize the allele specificity of *RPI1*, we swapped *RPI1* alleles between the strains. S288c $RPI1^{Sigma}$ displayed an adherence phenotype and *FLO11* RNA levels that were not significantly different from an *rpi1*Δ, suggesting that $RPI1^{Sigma}$ is not functional in *FLO11* regulation (Figure 4, A and B). Deletion of *TEC1* in S288c $RPI1^{Sigma}$ does not further decrease adhesion or *FLO11* levels. Reciprocally, the Sigma $RPI1^{S288c}$ strain had *FLO11* mRNA levels that were comparable to wild type, and when *TEC1* is deleted, Sigma $RPI1^{S288c}$ *tec1*Δ had more *FLO11* RNA than the Sigma $RPI1^{Sigma}$ *tec1*Δ, but less than wild type (Figure 4C). These results show that the $RPI1^{S288c}$ allele promotes *FLO11* expression and can partially bypass the *tec1*Δ; however, the $RPI1^{Sigma}$ allele is unable to bypass *tec1*Δ.

Rpi1p interaction with the FLO11 promoter is Rpi1p allele specific

To determine whether the difference in fMAPK-independent *FLO11* expression is a consequence of differences in the ability of $Rpi1p^{Sigma}$ and $Rpi1p^{S288c}$ to interact with the *FLO11* promoter, we performed ChIP and tested for enrichment of the *FLO11* promoter. $Rpi1p^{S288c}$ interacts with the *FLO11* promoter with a peak around −1300 bp (Figure 5A), the site bound by other positive activators of *FLO11* such as Tec1p, and Flo8p (Zeitlinger *et al.* 2003; Borneman *et al.* 2006). Immunoprecipitation of the $Rpi1p^{S288c}$ allele enriches for the *FLO11* promoter regardless of the strain background. In contrast to $Rpi1p^{S288c}$, immunoprecipitation of $Rpi1p^{Sigma}$ results in strain-background–specific enrichment for this same region of the *FLO11* promoter. When $Rpi1p^{Sigma}$ is immunoprecipitated from a Sigma strain, it enriches for the *FLO11* promoter; when it is immunoprecipitated from an S288c strain, it does not.

This difference between $Rpi1p^{S288c}$ and $Rpi1p^{Sigma}$ promoter binding is also observed at the promoter of *MIT1*, previously identified as a target of Rpi1p and a "master regulator" of *FLO11* transcription (Zeitlinger *et al.* 2003; Cain *et al.* 2011; Wang *et al.* 2011). However, Wang *et al.* and Cain *et al.* provided only strain-specific analyses of *MIT1* and *RPI1* function: The $Mit1p^{Sigma}$ protein was shown to bind to the *FLO11* promoter in Sigma, and $Rpi1p^{S288c}$ has been reported to localize to the promoter of $MIT1^{S288c}$ in S288c. Our ChIP data show that $Rpi1p^{S288c}$ localizes to the *MIT1* promoter, regardless of strain background, but $Rpi1p^{Sigma}$ localizes to the *MIT1* promoter only in the Sigma background (Figure 5B). Furthermore, $Rpi1p^{S288c}$ requires a functional *MIT1* to suppress a defect in the fMAPK pathway in both S288c and Sigma. $Rpi1p^{Sigma}$ can interact with both the *FLO11* and the *MIT1* promoters in Sigma, but not in S288c. Thus, $Rpi1p^{Sigma}$ must be structurally different from $Rpi1p^{S288c}$ and require additional factors to function.

The Rpi1p protein is differentially phosphorylated in the two strains

Analysis of the Rpi1p protein showed that $Rpi1p^{S288c}$ is structurally different from $Rpi1p^{Sigma}$. Figure 6 shows that 3× FLAG-tagged $Rpi1p^{S288c}$ extracted from S288c and visualized on Western blots runs as a diffuse species different from the $Rpi1p^{Sigma}$ band from Sigma. When $Rpi1p^{S288c}$ is expressed in Sigma, it again runs as a diffuse higher molecular weight species, but when $Rpi1p^{Sigma}$ is expressed in S288c, it runs as a single band (Figure 6).

To determine whether the difference between the isoforms of Rpi1p is due to phosphorylation, protein extracts were treated with λ-phosphatase. The broad $Rpi1p^{S288c}$ band collapsed to a single band. This change in migration pattern occurs regardless of the strain background that expresses $Rpi1p^{S288c}$. Treatment of $Rpi1p^{Sigma}$ with phosphatase changed its migration only if the protein was obtained from a Sigma strain. These experiments show that $Rpi1p^{Sigma}$ has strain-specific phosphorylation and likely has a different phosphorylation pattern from that of $Rpi1p^{S288c}$. This altered phosphorylation pattern of $Rpi1p^{Sigma}$ may account for its inability to activate *FLO11* transcription in either strain.

The RPI1 polymorphism is not restricted to laboratory strains

The striking difference in the control of *FLO11* transcription between these two strains could be attributed to their long-term culture in the laboratory. Indeed, all S288c strains have a nonsense mutation in *FLO8* and many have a mutation in the *KSS1* gene as well, both affecting *FLO11* expression (Elion *et al.* 1991; Liu *et al.* 1996). However, an assessment *RPI1* sequences shows that the S288c-like polymorphisms

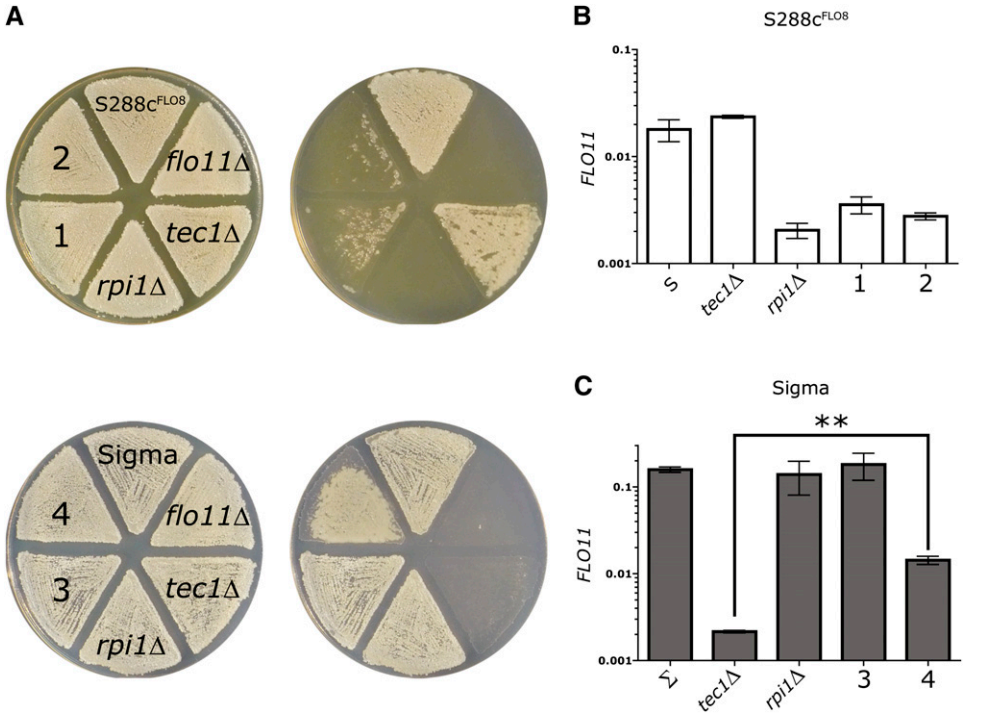

Figure 4 *RPI1*^{S288c} can partially bypass the fMAPK pathway for agar adhesion and *FLO11* expression. (A) Agar adhesion of S288c and Sigma strains carrying reciprocal allele swaps of *RPI1*. The top row shows adhesion assays performed on S288c strains grown on YPD and the bottom row shows adhesion assays performed on Sigma strains grown on synthetic media (see *Materials and Methods*). The same plates are shown before and after washing. (B and C) qPCR assay of *FLO11* transcript levels performed on (B) S288c strains grown in synthetic media and (C) Sigma strains grown on YPD. Mean *FLO11* levels normalized to *ACT1* levels are presented ± SD. $^{**}P < 0.01$. Strains with their endogenous *RPI1* allele are labeled with their relevant genotype. Strains carrying a swapped *RPI1* allele are labeled numerically: (1) S288c *RPI1*^{Sigma}; (2) S288c *RPI1*^{Sigma}, *tec1Δ*; (3) Sigma *RPI1*^{S288c}; and (4) Sigma *RPI1*^{S288c}, *tec1Δ*.

are widespread and found in both feral and laboratory strains (Figure S6). Thus, the expansion and contraction of *RPI1* appears to be a common avenue for diversity both in the laboratory and in the wild.

Intragenic tandem repeats are highly polymorphic within a species

The difference in repeat length between the *RPI1* alleles of S288c and Sigma led us to ask how many other genes differ in this way. Previous studies focused on cell surface proteins and have found profound phenotypic consequences for changes in the size of an internal repeat region (MacDonald *et al.* 1993; Verstrepen *et al.* 2005; Levdansky *et al.* 2007; Fidalgo *et al.* 2008; Tan *et al.* 2010; Sheets and St. Geme 2011), but it is difficult to perform genome-wide examinations of repeat length changes because few organisms have multiple genomes of sufficiently high quality to compare repeat regions. With the release of the Sigma genome, this comparison can be done because both the S288c and the Sigma genomes are of a high enough quality to ask, like in *RPI1*, how many genes differ in size due to repeat length changes? By computationally comparing the size of every ORF between S288c and Sigma, we identified 107 genes that differ in length due to in-frame expansions or contractions of intragenic repeat sequences (Table S4). The set of genes with intragenic repeat length differences includes genes involved in diverse biological processes, including transcription, chromatin modification, and signal transduction. To ensure that these differences are not due to sequencing errors, 24 of these length differences were verified by PCR (Figure 7 and Figure S7). Twenty-two of 24 genes show the predicted size difference, confirming the size differences predicted from the genome sequences' reflected length differences in the repeats.

Discussion

Individuals within a species may signal gene expression through different pathways

Our analysis of comparable deletion libraries in two interfertile strains of *S. cerevisiae* (Sigma and S288c) with nearly identical genomes (Dowell *et al.* 2010) allowed us to ask the question: Do the same signal transduction pathways control development in both strains? Previous mutational analyses identified the fMAPK pathway as required for adhesion and *FLO11* transcription in Sigma (Roberts and Fink 1994; Cook *et al.* 1996; Lorenz and Heitman 1998). A recent comprehensive genome-wide analysis of the Sigma deletion library for adhesion, filamentation, and biofilm formation again uncovered the fMAPK genes (Ryan *et al.* 2012). Therefore, the finding that S288c does not require the fMAPK pathway was unanticipated. This functional difference is not a consequence of gene duplication but rather involves distinct genes encoding two separate pathways, each capable of eliciting the same phenotype. The two strains differ by polymorphisms in the transcription factor *RPI1*; the *RPI1*^{S288c} allele is active and suppresses the loss of function of the fMAPK pathway; the *RPI1*^{Sigma} allele is inactive and incapable of suppressing of a defect in the fMAPK pathway. These *RPI1* polymorphisms must alter phosphorylation sites, change the conformation to prevent access to the sites, or prevent interaction with a kinase.

The discovery of *RPI1*^{S288c} as a bypass suppressor of the fMAPK pathway provides insight into the mechanism by

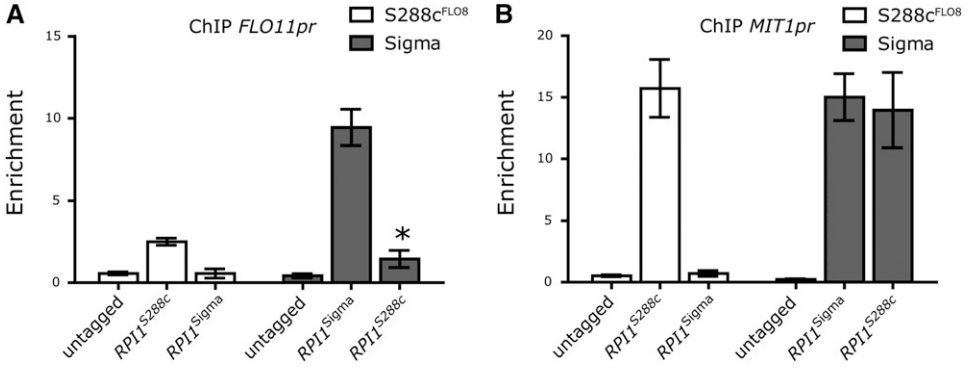

Figure 5 *RPI1*^{S288c} shows strain-independent localization to the *MIT1* and *FLO11* promoters. (A and B) Localization of Rpi1p using FLAG-tagged alleles in Sigma and S288c assayed by ChIP followed by qPCR for enrichment at (A) −1.3 kb in the *FLO11* promoter and (B) −1 kb in the *MIT1* promoter. Data were normalized to *ACT1* and are expressed as the mean fold enrichment ± SD. *$P < 0.01$ compared to untagged.

which allelic polymorphisms can buffer the effect of mutations and rewire a signaling pathway. Although previous studies have identified many QTL in intraspecies crosses of *S. cerevisiae*, many of these polymorphisms have not been connected to differences in function. As with the adhesion phenotype, each of the polymorphisms may have only a modest effect on the phenotype, making it difficult to isolate and assess the mechanism of action. We were able to tune the conditions so that we could use transformation to select for modifiers such as *RPI1* that only partially restore *FLO11* expression.

The presence of *RPI1*^{S288c} in S288c means that loss of function of any member of the fMAPK pathway will fail to manifest an adhesion phenotype because *FLO11* can now be activated by *RPI1*^{S288c}. Even *MSB2*, the protein believed to be the sensor for the fMAPK pathway, is not needed for S288c adhesion (Table S2). The activation of *FLO11* by *RPI1*^{S288c} raises the question: What is upstream of *RPI1* in S288c? Our genome-wide screen of the S288c library for strains with adhesion defects identified a number of potential candidates that do not have adhesion/filamentation defects in Sigma. In the future a systematic analysis of these is likely to identify those genes required for *RPI1* activation.

The evolution of circuit diversification begins within a species

Comparing species that evolved from a common ancestor before and after the whole-genome duplication (WGD) (Kellis *et al.* 2004; Wapinski *et al.* 2007) has elucidated the gradual rewiring of transcription circuits in the fungal lineage. For example, yeast species post-WGD have two proteins controlling the ribosomal protein stress response, a positive (*IFH1*) and a negative (*CRF1*) regulator, whereas organisms that did not undergo the WGD have a single ancestral protein with both positive and negative activities (Wapinski *et al.* 2010). Post-WGD, the duplicate genes specialized with one losing a positive function and the other a negative one, while both retained "stress response control."

The plasticity of these regulatory networks is most dramatically seen in the comparison of the regulatory circuit that regulates mating type in the human fungal pathogen *Candida albicans* with that of *S. cerevisiae*. The ensemble of genes controlling mating is largely conserved in the two organisms; however, the a-specific genes in *Candida* are under positive control by the a2 protein and in *S. cerevisiae* they are under negative control by the α2 protein. This transition from positive to negative regulation of the a-specific genes involved slight changes over evolutionary time in both the *cis*-acting elements in the promoters of the a-specific genes and the *trans*-acting regulatory proteins a2 and α2 (Tsong *et al.* 2006).

These variations in regulatory control observed in different species, which evolved over evolutionary time, must have arisen from variations that occurred within a single species and subsequently became fixed as sexual isolation took place. As we have shown, such variation in the circuitry of key signaling pathways exists among contemporary members of the same species. This apparent redundancy in *FLO11* activation raises the question: Why are the two pathways retained? Despite the overlapping functions of the fMAPK pathway and *RPI1*, the organization of these genes into complex networks likely imposes constraints on the loss of one or the other of these activation pathways. The elements of the fMAPK pathway that have been conserved in both S288c and Sigma (Ste20p, Ste11p, Ste7p, and Ste12p) are under strong positive selection because they have cross-pathway functions in additional signal transduction pathways (mating, osmotic sensing). Since *RPI1* regulates the cell wall under different conditions, it is also likely to function in conjunction with many pathways (Sobering *et al.* 2002; Puria *et al.* 2009; Wang *et al.* 2011). The finding that *RPI1* localizes not only to the *FLO11* promoter but also the *MIT1* promoter (Wang *et al.* 2011), itself a transcriptional activator of *FLO11* and many

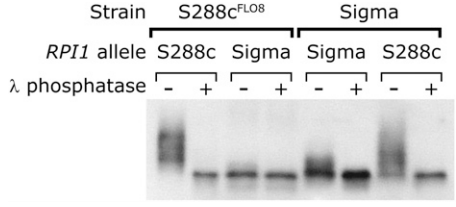

Figure 6 The Rpi1p^{S288c} protein is hyperphosphorylated. Shown is Western blot analysis of Rpi1p phosphorylation state in strains expressing either 3× flag-tagged *RPI1*^{S288c} or *RPI1*^{Sigma}. Samples were treated with either buffer or λ-phosphatase.

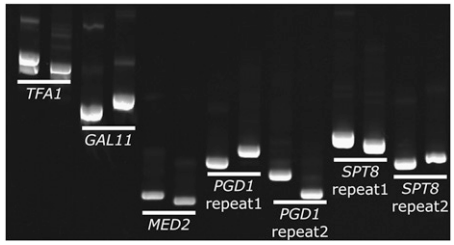

Figure 7 Many S288c genes differ from Sigma genes due to changes in intragenic tandem repeats. Twenty-four of the 107 genes predicted to differ between S288c and Sigma in the length of internal repeats were examined by PCR. Twenty-two of these genes had the predicted size difference. Five genes are shown and the results for the other genes are shown in Figure S7. *PGD1* and *SPT8* have two repeat regions that both change in size. For each pair the left sample is the S288c product and the right sample is the Sigma product.

other genes (Cain *et al.* 2011), is consistent with the idea that *RPI1* is also constrained by its participation in many regulatory networks.

RPI1^{S288c} and RPI1^{Sigma} differ by intragenic tandem repeat expansions

Although the two *RPI1* alleles differ by several nucleotide changes, the most striking difference is the alteration in the size of a repeat region present in the coding sequence of the gene. These repeat polymorphisms in *RPI1* are present in wild isolates of yeast as well as in many laboratory strains (Figure S6). Some wild isolates have the *RPI1^{S288c}* length repeat and others have the *RPI1^{Sigma}* length.

Repeats within a coding sequence create enormous flexibility for the evolution of diversity within a species. Because repeats can expand and contract at high frequencies, they permit a species to adapt to changing environments without becoming irreversibly committed to a phenotype (Rando and Verstrepen 2007). Although SNPs remain the major type of variation between S288c and Sigma, >100 genes differ in size due to repeat length differences. These data suggest that in a cross between S288c and Sigma these size polymorphisms could generate as many as 2^{100} genotypes in a cross. Phenotypic effects from even a tiny fraction of this variation, would provide ample grist for evolution's mill.

Acknowledgments

We thank William Timberlake for critical reading of this manuscript. This work was supported by National Institutes of Health grant GM035010. C.B. was supported by the Natural Sciences and Engineering Research Council of Canada and Howard Hughes Medical Institute.

Literature Cited

Borneman, A. R., J. A. Leigh-Bell, H. Yu, P. Bertone, M. Gerstein *et al.*, 2006 Target hub proteins serve as master regulators of development in yeast. Genes Dev. 20: 435–448.

Brem, R. B., G. Yvert, R. Clinton, and L. Kruglyak, 2002 Genetic dissection of transcriptional regulation in budding yeast. Science 296: 752–755.

Brown, T., 2001 *Southern Blotting in Current Protocols in Molecular Biology.* John Wiley & Sons, New York.

Bumgarner, S. L., R. D. Dowell, P. Grisafi, D. K. Gifford, and G. R. Fink, 2009 Toggle involving cis-interfering noncoding RNAs controls variegated gene expression in yeast. Proc. Natl. Acad. Sci. USA 106: 18321–18326.

Cain, C. W., M. B. Lohse, O. R. Homann, and A. D. Johnson, 2011 A conserved transcriptional regulator governs fungal morphology in widely diverged species. Genetics 190: 511–521.

Carlborg, O., and C. S. Haley, 2004 Epistasis: Too often neglected in complex trait studies? Nat. Rev. Genet. 5: 618–625.

Connelly, C. F., and J. M. Akey, 2012 On the prospects of whole-genome association mapping in *Saccharomyces cerevisiae*. Genetics 191: 1345–1353.

Cook, J. G., L. Bardwell, S. J. Kron, and J. Thorner, 1996 Two novel targets of the MAP kinase Kss1 are negative regulators of invasive growth in the yeast Saccharomyces cerevisiae. Genes Dev. 10: 2831–2848.

Demogines, A., E. Smith, L. Kruglyak, and E. Alani, 2008 Identification and dissection of a complex DNA repair sensitivity phenotype in Baker's yeast. PLoS Genet. 4: e1000123.

Dickson, S. P., K. Wang, I. Krantz, H. Hakonarson, and D. B. Goldstein, 2010 Rare variants create synthetic genome-wide associations. PLoS Biol. 8: e1000294.

Dowell, R. D., O. Ryan, A. Jansen, D. Cheung, S. Agarwala *et al.*, 2010 Genotype to phenotype: a complex problem. Science 328: 469.

Ehrenreich, I. M., N. Torabi, Y. Jia, J. Kent, S. Martis *et al.*, 2010 Dissection of genetically complex traits with extremely large pools of yeast segregants. Nature 464: 1039–1042.

Elion, E. A., J. A. Brill, and G. R. Fink, 1991 FUS3 represses CLN1 and CLN2 and in concert with KSS1 promotes signal transduction. Proc. Natl. Acad. Sci. USA 88: 9392–9396.

Fidalgo, M., R. R. Barrales, and J. Jimenez, 2008 Coding repeat instability in the FLO11 gene of Saccharomyces yeasts. Yeast 25: 879–889.

Gatbonton, T., M. Imbesi, M. Nelson, J. M. Akey, D. M. Ruderfer *et al.*, 2006 Telomere length as a quantitative trait: genome-wide survey and genetic mapping of telomere length-control genes in yeast. PLoS Genet. 2: e35.

Gimeno, C. J., P. O. Ljungdahl, C. A. Styles, and G. R. Fink, 1992 Unipolar cell divisions in the yeast S. cerevisiae lead to filamentous growth: regulation by starvation and RAS. Cell 68: 1077–1090.

Graham, T. R., 2001 Metabolic labeling and immunoprecipitation of yeast proteins, pp. 7.6.1–7.6.9 in *Current Protocols in Cell Biology,* edited by J. S. Bonifacino, M. Dasso, J. B. Harford, J. Lippincott-Schwartz, and K. M. Yamada. John Wiley & Sons, New York.

Guthrie, C., and G. Fink, 2002 *Guide to Yeast Genetics and Molecular and Cellular Biology.* Academic Press, San Diego, CA.

Halme, A., S. Bumgarner, C. Styles, and G. R. Fink, 2004 Genetic and epigenetic regulation of the FLO gene family generates cell-surface variation in yeast. Cell 116: 405–415.

Hartman, J. L., IV, B. Garvik, and L. Hartwell, 2001 Principles for the buffering of genetic variation. Science 291: 1001–1004.

Jakobsdottir, J., M. B. Gorin, Y. P. Conley, R. E. Ferrell, and D. E. Weeks, 2009 Interpretation of genetic association studies: markers with replicated highly significant odds ratios may be poor classifiers. PLoS Genet. 5: e1000337.

Kellis, M., N. Patterson, M. Endrizzi, B. Birren, and E. S. Lander, 2003 Sequencing and comparison of yeast species to identify genes and regulatory elements. Nature 423: 241–254.

Kellis, M., B. W. Birren, and E. S. Lander, 2004 Proof and evolutionary analysis of ancient genome duplication in the yeast Saccharomyces cerevisiae. Nature 428: 617–624.

Korbel, J. O., A. E. Urban, J. P. Affourtit, B. Godwin, F. Grubert *et al.*, 2007 Paired-end mapping reveals extensive structural variation in the human genome. Science 318: 420–426.

Lee, T. I., S. E. Johnstone, and R. A. Young, 2006 Chromatin immunoprecipitation and microarray-based analysis of protein location. Nat. Protoc. 1: 729–748.

Levdansky, E., J. Romano, Y. Shadkchan, H. Sharon, K. J. Verstrepen *et al.*, 2007 Coding tandem repeats generate diversity in Aspergillus fumigatus genes. Eukaryot. Cell 6: 1380–1391.

Liti, G., D. M. Carter, A. M. Moses, J. Warringer, L. Parts *et al.*, 2009 Population genomics of domestic and wild yeasts. Nature 458: 337–341.

Liu, H., C. A. Styles, and G. R. Fink, 1993 Elements of the yeast pheromone response pathway required for filamentous growth of diploids. Science 262: 1741–1744.

Liu, H., C. A. Styles, and G. R. Fink, 1996 Saccharomyces cerevisiae S288C has a mutation in FLO8, a gene required for filamentous growth. Genetics 144: 967–978.

Lo, W. S., and A. M. Dranginis, 1998 The cell surface flocculin Flo11 is required for pseudohyphae formation and invasion by Saccharomyces cerevisiae. Mol. Biol. Cell 9: 161–171.

Lorenz, M. C., and J. Heitman, 1998 Regulators of pseudohyphal differentiation in Saccharomyces cerevisiae identified through multicopy suppressor analysis in ammonium permease mutant strains. Genetics 150: 1443–1457.

MacDonald, M. E., C. M. Ambrose, M. P. Duyao, R. H. Myers, C. Lin *et al.*, 1993 A novel gene containing a trinucleotide repeat that is expanded and unstable on Huntington's disease chromosomes. Cell 72: 971–983.

Manolio, T. A., F. S. Collins, N. J. Cox, D. B. Goldstein, L. A. Hindorff *et al.*, 2009 Finding the missing heritability of complex diseases. Nature 461: 747–753.

Nogami, S., Y. Ohya, and G. Yvert, 2007 Genetic complexity and quantitative trait loci mapping of yeast morphological traits. PLoS Genet. 3: e31.

Puria, R., M. A. Mannan, R. Chopra-Dewasthaly, and K. Ganesan, 2009 Critical role of RPI1 in the stress tolerance of yeast during ethanolic fermentation. FEMS Yeast Res. 9: 1161–1171.

Rando, O. J., and K. J. Verstrepen, 2007 Timescales of genetic and epigenetic inheritance. Cell 128: 655–668.

Rice, P., I. Longden, and A. Bleasby, 2000 EMBOSS: the European Molecular Biology Open Software Suite. Trends Genet. 16: 276–277.

Roberts, R. L., and G. R. Fink, 1994 Elements of a single MAP kinase cascade in Saccharomyces cerevisiae mediate two developmental programs in the same cell type: mating and invasive growth. Genes Dev. 8: 2974–2985.

Rose, M. D., P. Novick, J. H. Thomas, D. Botstein, and G. R. Fink, 1987 A Saccharomyces cerevisiae genomic plasmid bank based on a centromere-containing shuttle vector. Gene 60: 237–243.

Rozen, S., and H. Skaletsky, 2000 Primer3 on the WWW for general users and for biologist programmers. Methods Mol. Biol. 132: 365–386.

Ryan, O., R. S. Shapiro, C. F. Kurat, D. Mayhew, A. Baryshnikova *et al.*, 2012 Global gene deletion analysis exploring yeast filamentous growth. Science 337: 1353–1356.

Schacherer, J., J. A. Shapiro, D. M. Ruderfer, and L. Kruglyak, 2009 Comprehensive polymorphism survey elucidates population structure of Saccharomyces cerevisiae. Nature 458: 342–345.

Sheets, A. J., and J. W. St. Geme, III, 2011 Adhesive activity of the haemophilus cryptic genospecies cha autotransporter is modulated by variation in tandem peptide repeats. J. Bacteriol. 193: 329–339.

Sobering, A. K., U. S. Jung, K. S. Lee, and D. E. Levin, 2002 Yeast Rpi1 is a putative transcriptional regulator that contributes to preparation for stationary phase. Eukaryot. Cell 1: 56–65.

Tan, J. C., A. Tan, L. Checkley, C. M. Honsa, and M. T. Ferdig, 2010 Variable numbers of tandem repeats in Plasmodium falciparum genes. J. Mol. Evol. 71: 268–278.

Tsong, A. E., B. B. Tuch, H. Li, and A. D. Johnson, 2006 Evolution of alternative transcriptional circuits with identical logic. Nature 443: 415–420.

Verstrepen, K. J., A. Jansen, F. Lewitter, and G. R. Fink, 2005 Intragenic tandem repeats generate functional variability. Nat. Genet. 37: 986–990.

Voynov, V., K. J. Verstrepen, A. Jansen, V. M. Runner, S. Buratowski *et al.*, 2006 Genes with internal repeats require the THO complex for transcription. Proc. Natl. Acad. Sci. USA 103: 14423–14428.

Wang, H., D. Mayhew, X. Chen, M. Johnston, and R. D. Mitra, 2011 Calling cards enable multiplexed identification of the genomic targets of DNA-binding proteins. Genome Res. 21: 748–755.

Wapinski, I., A. Pfeffer, N. Friedman, and A. Regev, 2007 Natural history and evolutionary principles of gene duplication in fungi. Nature 449: 54–61.

Wapinski, I., J. Pfiffner, C. French, A. Socha, D. A. Thompson *et al.*, 2010 Gene duplication and the evolution of ribosomal protein gene regulation in yeast. Proc. Natl. Acad. Sci. USA 107: 5505–5510.

Winzeler, E. A., D. D. Shoemaker, A. Astromoff, H. Liang, K. Anderson *et al.*, 1999 Functional characterization of the S. cerevisiae genome by gene deletion and parallel analysis. Science 285: 901–906.

Winzeler, E. A., H. Liang, D. D. Shoemaker, and R. W. Davis, 2000 Functional analysis of the yeast genome by precise deletion and parallel phenotypic characterization. Novartis Found. Symp. 229: 105–109, discussion 109–111.

Wolf, J. J., R. D. Dowell, S. Mahony, M. Rabani, D. K. Gifford *et al.*, 2010 Feed-forward regulation of a cell fate determinant by an RNA-binding protein generates asymmetry in yeast. Genetics 185: 513–522.

Zeitlinger, J., I. Simon, C. T. Harbison, N. M. Hannett, T. L. Volkert *et al.*, 2003 Program-specific distribution of a transcription factor dependent on partner transcription factor and MAPK signaling. Cell 113: 395–404.

Communicating editor: C. D. Jones

GENETICS

Supporting Information
http://www.genetics.org/lookup/suppl/doi:10.1534/genetics.112.145573/-/DC1/

Genetic Variation in *Saccharomyces cerevisiae*: Circuit Diversification in a Signal Transduction Network

Brian L. Chin, Owen Ryan, Fran Lewitter, Charles Boone, and Gerald R. Fink

DOI: 10.1534/genetics.112.145573

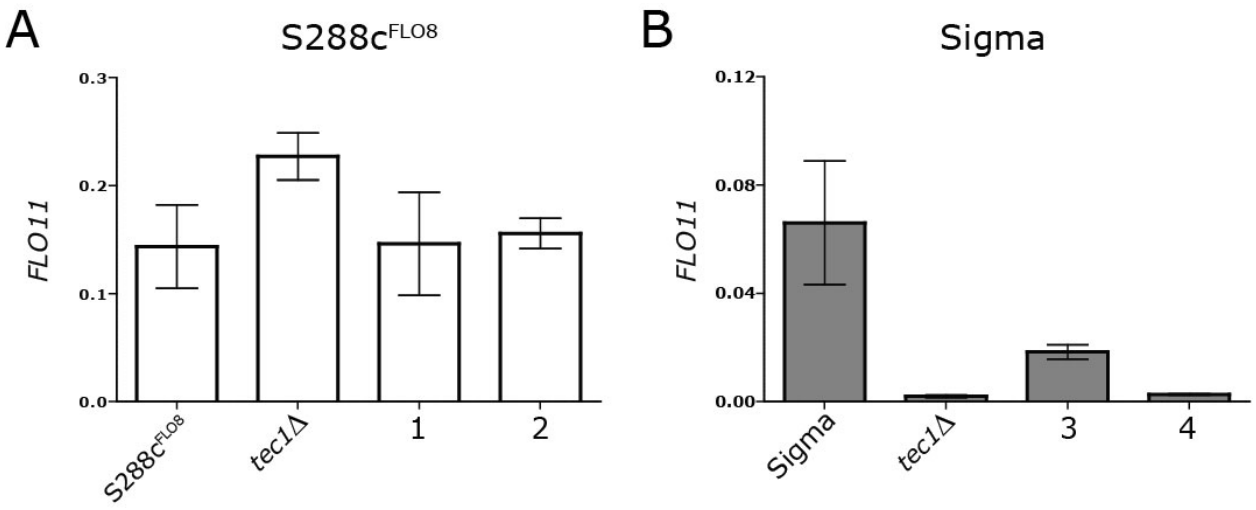

Figure S1 S288c with *FLO11pr*^{Sigma}*::FLO11* is still fMAPK independent. qPCR assay of *FLO11* transcript levels was performed on (A) S288c and (B) Sigma strains carrying *FLO11* promoter swaps. Mean *FLO11* levels normalized to *ACT1* levels are presented ± SD. Strains with their endogenous *FLO11* promoter are labeled with their relevant genotype. Strains carrying a swapped *FLO11* promoter are labeled numerically: (1) S288c *FLO11pr*^{Sigma}*::FLO11*; (2) S288c *FLO11pr*^{Sigma}*::FLO11, tec1Δ*; (3) Sigma *FLO11pr*^{S288c}*::FLO11*; (4) Sigma *FLO11pr*^{S288c}*::FLO11*, *tec1Δ*.

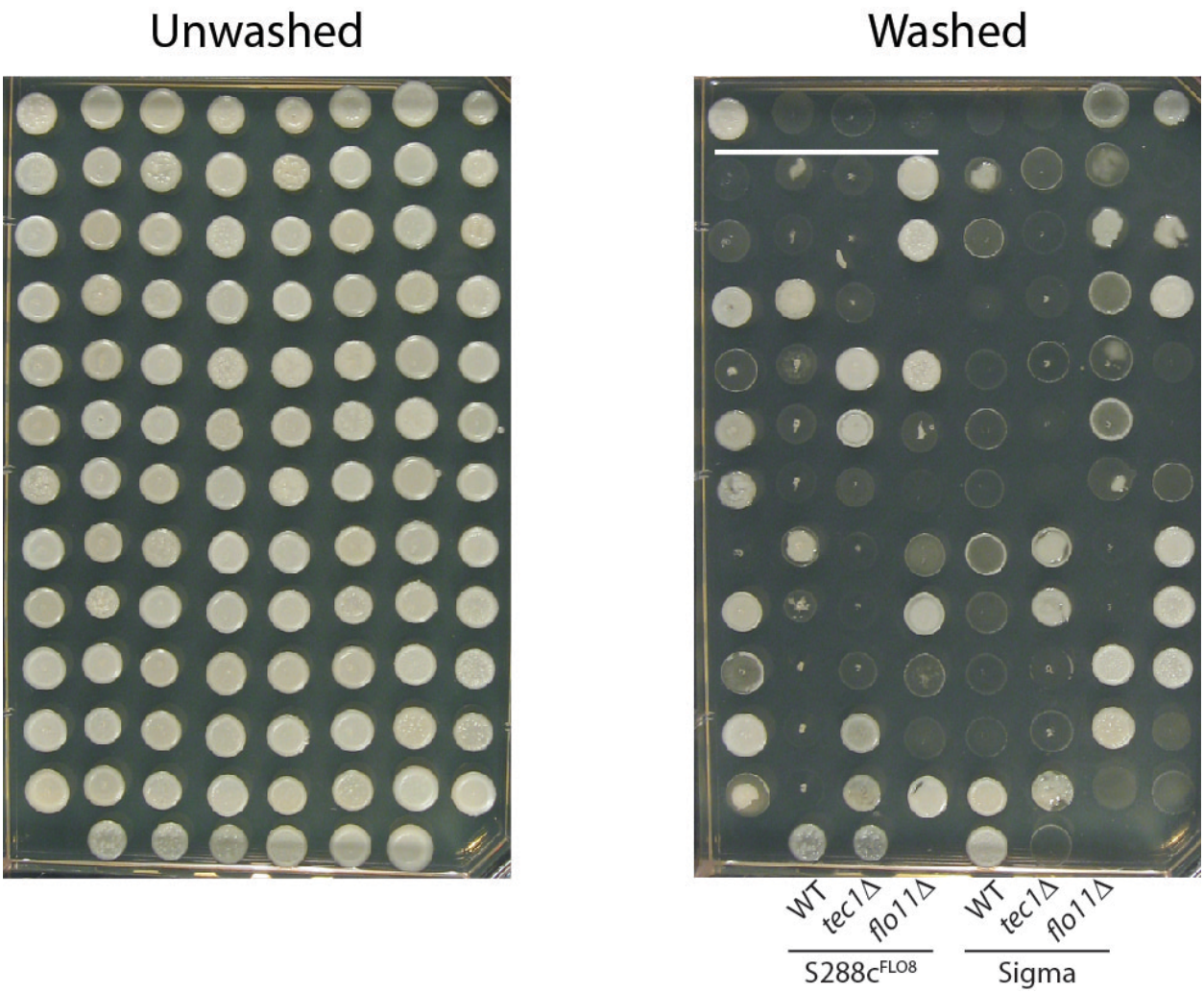

Figure S2 *tec1Δ* bypass is a complex trait. Agar adhesion assays of 24 tetrads from an S288c *tec1Δ* x Sigma *tec1Δ* cross. Two complete tetrads per row with one example underlined. Parental strains and controls spotted on the bottom of the plate. The same plate is shown before and after washing.

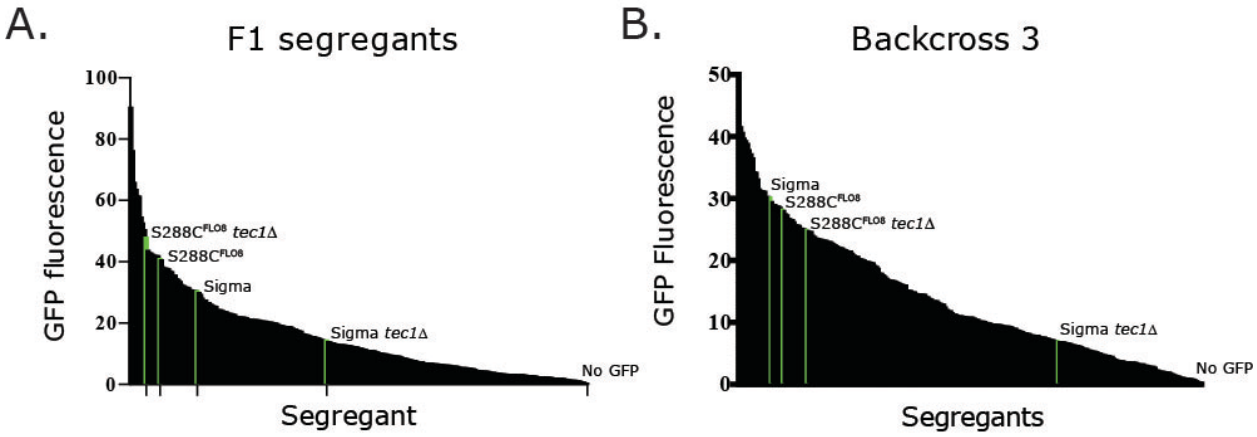

Figure S3 fMAPK bypass of *FLO11* expression is a complex quantitative trait. GFP fluorescence, measured in arbitrary units for (A) 276 F1 meiotic progney from a S288c / Sigma *FLO11pr::GFP* / *FLO11pr::GFP tec1Δ* / *tec1Δ* diploid or (B) 276 meiotic progeny from the third generation of backcrossing (see methods). The average GFP fluorescence normalized to OD600 of 3 biological replicates are plotted. The progeny are sorted from highest to lowest fluorescence. Fluorescence of control strains are labeled and shown in green.

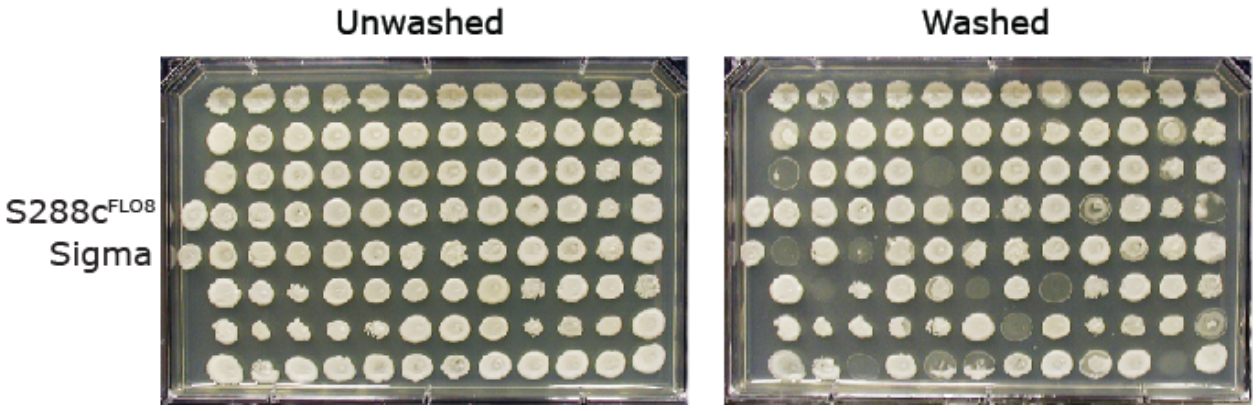

Figure S4 Regulation of adhesion differs between S288c and Sigma. Adherent, wild-type S288c and Sigma were crossed and from 24 complete tetrads, 15/96 progeny show an adhesion defect. Each column contains two complete tetrads.

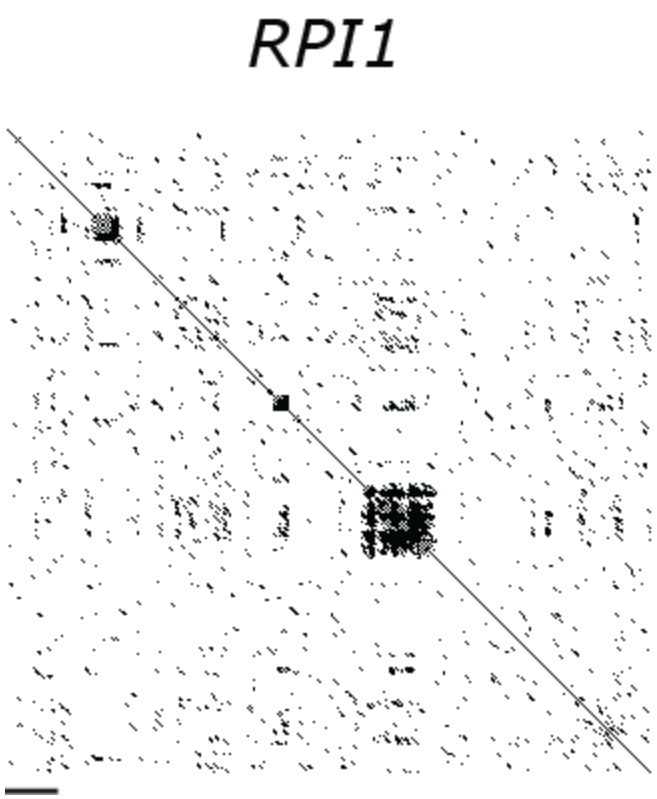

Figure S5 *RPI1* contains intragenic repeats. Dot plot analysis of the S288c allele of *RPI1* nucleotide sequence compared against itself. Repeat regions produce a characteristic box pattern. The horizontal bar represents 100 nt. The plot was generated using http://www.vivo.colostate.edu/molkit/dnadot/ with a windows size of 9 and a mismatch limit of 2.

A

Repeat #1

```
S288c   TCCAGTTCAAATTCGAATTCGAACTCCAATTCTAATTCGAACTCCAACTCCAAC
w303    TCCAGTTCAAATTCGAATTCGAACTCCAATTCTAATTCGAACTCCAACTCCAAC
SK1     TCCAGTTCAAATTCGAATTCGAACTCCAATTCTAATTCGAACTCCAACTCCAAC
NCYC110 TCCAGTTCAAATTCGAATTCGAACTCCAATTCTAATTCGAACTCCAACTCCAAC
YJM789  TCCAGTTCAAATTCGAATTCGAACTCCAATTCTAATTCGAACTCCAACTCCAAC
RM11    TCCAGTTCTAATTCTAATTCGAACTCCAACTCCAAC------------------
y55     TCCAGTTCTAATTCTAATTCGAACTCCAACTCCAAC------------------
Sigma   TCCAGTTCTAATTCTAATTCGAACTCCAACTCCAAC------------------
         S  S  S  N  S  N  S  N  S  N  S  N  S  N  S  N  S  N
```

B

Repeat #2

```
S288c   AACAAGAATGGTACTAATGATAATATTAATAACCATTATTATAATAATTGTAACAATAACAATAATAATATTAA----------------------------------------------CAATAGTAACAATAGCAACAATAATAATAGCAATAATATTAATAGGAATAGTAATCATAGTACTAAT
w303    AACAAGAATGGTACTAATGATAATATTAATAACCATTATTATAATAATTGTAACAATAACAATAATAATATTAA----------------------------------------------CAATAGTAACAATAGCAACAATAATAATAGCAATAATATTAATAGGAATAGTAATCATAGTACTAAT
SK1     AACAAGAATGGTACTAATGATAATATTAATAACCATTATTATAATAATAGTAACAATAACAATAATAATATTAA----------------------------------------------CAATAGTAACAATAGCAACAATAATAATAGCAATAATATTAATAGGAATAGTAATCATAGTACTAAT
NCYC110 AACAAGAATGGTACTAATGATAATATTAATAACCATTATTATAATAATAGTAACAATAACAATAATAATATTAA----------------------------------------------CAATAGTAACAATAGCAACAATAATAATAGCAATAATATTAATAGGAATAGTAATCATAGTACTAAT
YJM789  AACAAGAATGGTACTAATGATAATATTAATAACCATTATTATAATAATAGTAACAATAACAATAATAATATTAA---CAATAGTAACAATAATAA----------------------------TAATAGTAACAATAGCAACAATAATAATAGCAATAATATTAATAGGAATAGTAATCATAGTACTAAT
RM11    AACAAGAATGGTACTAATGATAATATTAATAACCATTATTATAATAATAGTAACAATAACAATAATAATAATAATAATTAACAATAGTAA----------------------------------CAATAATAATAATAGTAACAATAATAATAGCAATAATATTAATAGGAATAGTAATCATAGTACTAAT
y55     AACAAGAATGGTACTAATGATAATATTAATAACCATTATTATAATAATAGTAACAATAACAATAATAATAATAATAATTAACAATAGTAACAATAATAATAATAGTAA----------------CAATAATAATAATAGTAACAATAATAATAGCAATAATATTAATAGGAATAGTAATCATAGTACTAAT
Sigma   AACAAGAATGGTACTAATGATAATATTAATAACCATTATTATAATAATAGTAACAATAACAATAATAATAATAATAATTAACAATAGTAACAATAATAATAATAGTAACAATAATAATAATAGTAACAATAATAATAGCAATAATATTAATAGGAATAGTAATCATAGTACTAAT
          N  K  N  G  T  N  D  N  I  N  N  H  Y  Y  N  N  S  N  N  N  N  N  N  N  N  N  S  N  N  N  N  N  S  N  N  N  N  N  S  N  N  N  N  N  S  N  N  N  N  N  S  N  N  I  N  R  N  S  N  H  S  T  N
```

Figure S6 Comparison of *RPI1* repeat regions between different *S. cerevisiae* strains. The sequences for the repeat regions from *RPI1* were aligned using ClustalW. (A) 5' repeat region and (B) central repeat region. For repeat #1 the translation for the S288c sequence is shown, and for repeat #2 the translation for the Sigma sequence is shown. Strain names in blue are wild isolates and nucleotides in red represent nucleotide polymorphisms. In S288c, the repeats account for 16% of the coding sequence (195/1224 bases). The 5' repeat region consists of a hexanucleotide repeat. In S288c there are nine repeated units while in Sigma there are only six repeated units. The central repeat region consists of a trinucleotide repeat. In S288c there are 46 repeated units but in Sigma they have expanded to 63 repeated units. Both repeats encode primarily for serines and asparagines.

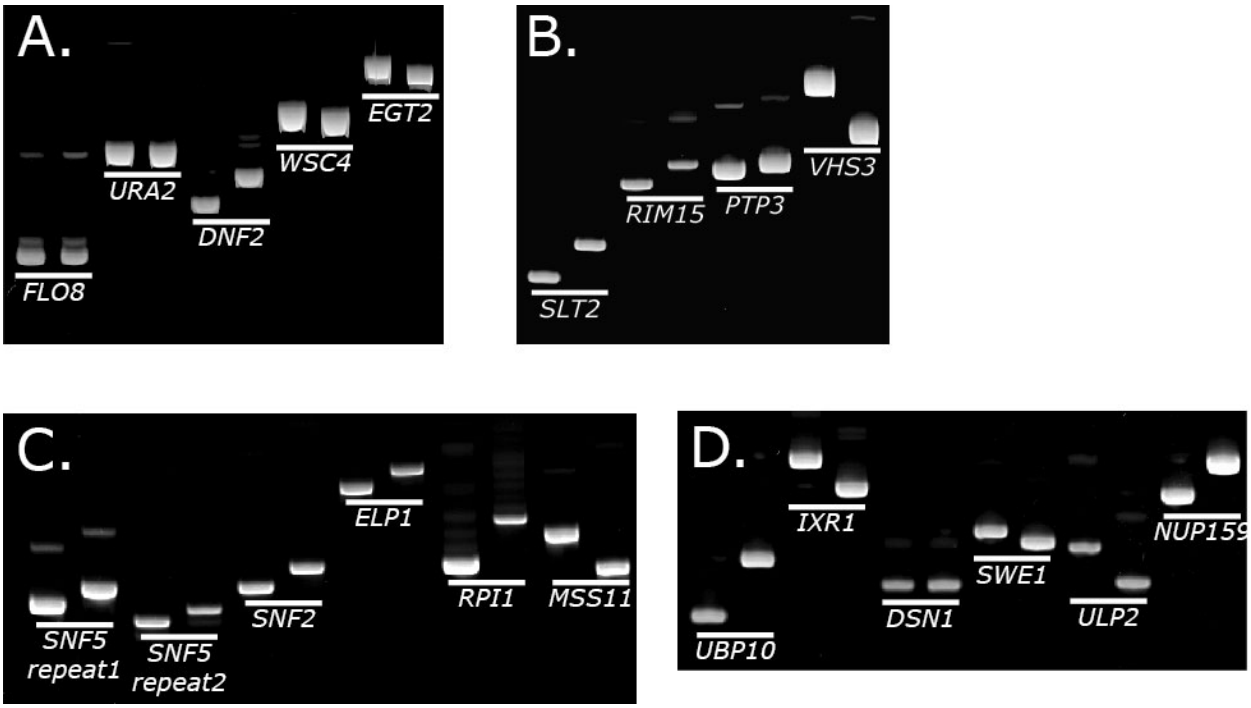

Figure S7 Many genes have intragenic tandem repeats that differ in size between S288c and Sigma. Four of five gels used to examine the length differences between S288c and Sigma for 24 genes and *FLO8* which was used as a control for a gene without repeats. 22/24 genes had the predicted repeat length differences. The gene *SNF5* has two repeat regions that both changed in size. For each pair the left sample is S288c and the right sample is Sigma.

Table S1 Deletions leading to an Ahs- phenotype only in S288c.

YAL054C	YIR020C	YOR082C	YBR231C
YNL020C	YJL218W	YOR154W	YBR289W
YOR043W	YJR018W	YOR183W	YDR073W
YDR226W	YJR054W	YOR186W	YDR334W
YBL080C	YJR080C	YOR200W	YJL176C
YKR039W	YKL023W	YOR225W	YOR290C
YBR068C	YKL044W	YOR258W	YOL012C
YDR127W	YKL090W	YOR285W	YDL074C
YPR060C	YKL094W	YPL017C	YDR469W
YPR020W	YLL030C	YPL068C	YDR207C
YLR431C	YLL055W	YPL182C	YBR107C
YCR002C	YLR021W	YPL184C	YDR254W
YAR030C	YLR065C	YPL216W	YDR318W
YBL031W	YLR125W	YPL220W	YGR275W
YBL046W	YLR168C	YPL246C	YPR046W
YBR033W	YLR184W	YPL257W	YER068W
YBR139W	YLR352W	YPL260W	YAL012W
YCL005W	YLR358C	YPR170C	YER056C
YCL036W	YLR374C	YER086W	YMR032W
YCR016W	YLR434C	YDR200C	YNL166C
YCR095C	YML010C-B	YCL058C	YNL229C
YDL021W	YML010W-A	YBL006C	YLR420W
YDL073W	YMR135W-A	YPR030W	YML106W
YDR003W	YMR158C-B	YER083C	YJL115W
YDR248C	YMR191W	YCR017C	YOL090W
YDR514C	YMR316C-A	YGL027C	YLR418C
YER039C	YMR326C	YHR181W	YBR228W
YER048C	YNL023C	YDL225W	YGL058W
YER060W	YNL170W	YBR200W	YML021C
YFL015C	YNL175C	YHL003C	YOR144C
YGL214W	YNL226W	YLL026W	YDR364C
YGR071C	YNR025C	YJR060W	YCL061C
YHL017W	YOL032W	YDR176W	YMR048W
YHR080C	YOL042W	YGL066W	YBL082C
YHR210C	YOL048C	YLR055C	YKL213C
YIL059C	YOL159C	YNL107W	YDR069C
YIL086C	YOR021C	YDR485C	YDR320C
YIR014W	YOR029W	YML041C	YNR006W

YJL095W
YKR054C
YBR159W
YBR171W
YGR135W
YFL011W
YHR094C
YBR133C
YOR178C
YNL117W
YLR330W
YJL062W
YDL035C
YOR101W
YKR029C
YOL064C
YGL045W
YHL007C
YOL101C
YKR042W
YOL091W
YDL115C
YLR219W
YML128C
YMR167W
YMR031W-A
YJR051W
YLR180W
YGR163W
YAL047C
YPL241C
YLR368W
YDR258C
YNL076W
YCL016C
YDR378C
YKL009W
YMR125W
YBR034C

YDR432W
YDR195W
YGR019W
YPR101W
YJR117W
YPR049C
YOL044W
YGR004W
YNL173C
YER053C
YFL031W
YAL013W
YDR174W
YNR052C
YKL043W
YJL129C
YDL230W
YJL183W
YKL139W
YIL148W
YGL236C
YCL037C
YDR500C
YHL033C
YKL167C
YLR185W
YNL265C
YOR096W
YOR182C
YPL090C
YOR138C
YHR034C
YOR288C
YMR091C
YER110C
YGL153W
YIR004W
YLR024C
YGL203C

YPR087W
YER020W
YML035C
YBR221C
YIL119C
YKL109W
YAL024C
YER059W
YPL219W
YMR179W
YML014W
YOL105C
YOR008C
YGL244W
YHR087W
YNR060W
YBL075C
YGR055W
YGL033W
YLR453C
YGR104C
YHR041C
YPL144W
YPL258C
YNL248C
YJL189W
YGR054W
YNL125C
YOR081C
YPL212C
YDR354W
YKL211C
YCL075W
YDR330W
YHL016C
YPR036W
YLR373C
YMR174C
YHL019C

YBR053C

Table S2 Deletions leading to an Ahs- phenotype only in Sigma.

YKR024C	YGR162W	YPL031C	YIR021W
YHR114W	YAL048C	YDL044C	YER161C
YML022W	YPL259C	YBR191W	YGR123C
YLR278C	YLR370C	YGR105W	YDL069C
YGL258W	YNL271C	YKL119C	YDR197W
YGR271C-A	YMR267W	YOR085W	YML024W
YML117W	YDR079W	YNR051C	YBR165W
YOR267C	YDR529C	YEL059C-A	YER154W
YMR044W	YPL132W	YPL086C	YLR384C
YOR213C	YLR204W	YPL024W	YDR074W
YMR127C	YLR315W	YIL008W	YHL034C
YCR009C	YER156C	YFR019W	YDR096W
YCR088W	YLR375W	YPL193W	YDL081C
YIL034C	YFR048W	YJL124C	YOL023W
YMR008C	YGL188C-A	YPR040W	YIL125W
YGR040W	YGL211W	YDR512C	YDR120C
YGL014W	YGL228W	YNL098C	YGR020C
YDR005C	YKL037W	YOL051W	YOR332W
YNL053W	YOR141C	YDR289C	YFL054C
YOR002W	YKL110C	YGR257C	YGR272C
YOR067C	YDR276C	YLL041C	YBR026C
YDL159W	YBL007C	YNL037C	YHR011W
YGL019W	YBR245C	YOR136W	YCR105W
YGR188C	YGR062C	YEL051W	YPR116W
YLR362W	YLR337C	YKL080W	YCR079W
YHR021C	YLR056W	YDL067C	YER014C-A
YPR043W	YGR014W	YLR295C	YLR390W-A
YBR189W	YGR037C	YBL099W	YGR229C
YGR232W	YHL038C	YDR298C	YDR359C
YER118C	YGL252C	YBL066C	YLR385C
YMR312W	YAL002W	YBR162C	YOL068C
YPL101W	YOR334W	YLR404W	YMR263W
YKL143W	YOL115W	YNL097C	YCR077C
YDR184C	YGL003C	YGR180C	YHR120W
YDL190C	YPL005W	YCR086W	YER061C
YEL060C	YDR140W	YDR129C	YHR067W
YDL005C	YAL023C	YML008C	YBL071W-A
YGL025C	YDR477W	YGL084C	YER014W

YEL065W
YOR198C
YPL055C
YDR393W
YHL020C
YGL246C
YER117W
YDL191W
YGL129C
YMR158W
YPL104W
YPR166C
YDR175C
YPL040C
YPL118W
YLR192C
YJL180C
YER017C
YMR089C
YNL121C
YPL148C
YIL049W
YNL119W
YHR084W
YHR111W
YIR019C
YFL026W
YNL180C
YDR194C
YKL149C
YKL194C
YPR163C
YBR127C
YMR293C
YKL055C
YOR221C
YPL271W
YDR332W
YOR305W

YBR163W
YER087W
YGL107C
YGR102C
YMR066W
YMR098C
YOR205C
YLR443W
YIL084C
YOR330C
YLR382C
YKL134C
YNL073W
YGR171C
YCR028C-A
YDR296W
YOL095C
YGL219C
YNL213C
YGR101W
YLL006W
YOL009C
YOR211C
YML062C
YLR435W
YDL090C
YBR146W
YBL038W
YBR251W
YBR268W
YBR282W
YCR003W
YCR024C
YCR046C
YCR071C
YDL045W-A
YDR237W
YDR322W
YDR347W

YDR405W
YER050C
YGR215W
YHR147C
YHR168W
YIL093C
YKL003C
YKL138C
YKL155C
YKL170W
YKR006C
YLR312W-A
YLR439W
YMR024W
YMR193W
YNL005C
YNL081C
YNL252C
YPL173W
YPR047W
YBL090W
YDR115W
YDR337W
YEL050C
YGL143C
YGR165W
YGR220C
YHR091C
YJL063C
YKR085C
YLR139C
YMR097C
YNL177C
YOR150W
YPR100W
YPL002C
YBL022C
YBR083W
YGL064C

YMR287C
YPL029W
YML055W
YLL033W
YMR228W
YJL102W
YLR069C
YOR187W
YDR470C
YDR268W
YPL097W
YPL019C
YGR219W
YAL004W

Table S3 Deletions leading to an Ahs- phenotype only in both S288c and Sigma.

YKL007W
YBR023C
YPL203W
YBL058W
YGR056W
YOL001W
YOL072W
YLR357W
YOL076W
YPL181W
YDR350C
YMR154C

YKR001C
YKL185W
YNL183C
YDR392W
YOR035C
YJL140W
YHR167W
YKL204W
YJR113C
YCL008C
YJR102C
YOL004W

YDR065W
YMR116C
YDL233W
YEL007W
YGR122W
YBR095C
YOR275C
YOR030W
YLR025W
YMR077C
YCR084C
YDL006W

YDR462W
YNR037C
YLR417W
YMR164C
YGR200C
YGR063C
YMR063W
YHL027W
YNL294C
YJL175W

Table S4 ORFs with intragenic repeat length differences between S288c and Sigma.

YAL035W
YAL064W-B
YBL011W
YBR017C
YBR030W
YBR212W
YCR067C
YDL005C
YDL035C
YDL122W
YDR133C
YDR134C
YDR232W
YDR273W
YDR299W
YEL007W
YFL024C
YFL033C
YGL013C
YGL237C
YGR014W
YHL020C
YHR030C
YJL187C
YKL023W
YKL108W
YKL163W
YKR072C
YLL008W
YLR175W
YLR330W
YML074C
YMR070W
YMR136W
YMR164C
YNL186W
YOL051W
YOR053W

YOR156C
YOR290C
YPL049C
YPL229W
YPR142C
YPR143W
YPR152C
YAL065C
YAR050W
YBR289W
YCL043C
YDL037C
YDL039C
YDL058W
YDR093W
YDR150W
YDR420W
YDR517W
YER011W
YER030W
YER075C
YFL010C
YFL010W-A
YGL014W
YGR160W
YHL028W
YHR077C
YIL011W
YIL031W
YIL115C
YIL119C
YIR010W
YIR019C
YIR023W
YJL020C
YJL078C
YJL123C
YJL130C

YJL162C
YKL028W
YKL032C
YKL105C
YKR092C
YKR102W
YLL010C
YLR055C
YLR106C
YLR114C
YLR177W
YLR406C-A
YML049C
YML113W
YMR016C
YMR044W
YMR124W
YMR173W
YMR173W-A
YMR317W
YNL271C
YNL327W
YNR052C
YOR010C
YOR054C
YOR113W
YOR267C
YPL216W
YPR021C
YPR123C
YPR124W

Table S5 List of strains used in this study

Strain	Genotype	Source
BY4741	S288c *MAT***a** *his3Δ*1 *leu2Δ*0 *ura3Δ*0 *met15Δ*0 *flo8*-1	Brachmann et al. (1998)
yBC37	S288c *MAT***a** *his3Δ*1 *leu2Δ*0 *ura3Δ*0 *met15Δ*0 *FLO8*	this study
yBC06A10	S288c *MAT***a** *his3Δ*1 *leu2Δ*0 *ura3Δ*0 *met15Δ*0 *FLO8 tec1Δ*::KanMX4	this study
yBC06B5	S288c *MAT***a** *his3Δ*1 *leu2Δ*0 *ura3Δ*0 *met15Δ*0 *FLO8 ste7Δ*::KanMX4	this study
yBC06G7	S288c *MAT***a** *his3Δ*1 *leu2Δ*0 *ura3Δ*0 *met15Δ*0 *FLO8 ste11Δ*::KanMX4	this study
yBC07A3	S288c *MAT***a** *his3Δ*1 *leu2Δ*0 *ura3Δ*0 *met15Δ*0 *FLO8 kss1Δ*::KanMX4	this study
yBC06B5	S288c *MAT***a** *his3Δ*1 *leu2Δ*0 *ura3Δ*0 *met15Δ*0 *FL*O8 ste12Δ::KanMX4	this study
yBC0192	S288c *MAT***a** *his3Δ*1 *leu2Δ*0 *ura3Δ*0 *met15Δ*0 *flo11*pr^{S288c}*Δ*::*FLO11*pr^{Sigma} *FLO8*	this study
yBC0195	S288c *MAT***a** *his3Δ*1 *leu2Δ*0 *ura3Δ*0 *met15Δ*0 *flo11*pr^{S288c}*Δ*::*FLO11*pr^{Sigma}*tec1Δ*::KanMX4 *FLO8*	this study
yBC11E2	S288c *MAT***a** *his3Δ*1 *leu2Δ*0 *ura3Δ*0 *met15Δ*0 *flo11Δ*::GFP-*URA3 FLO8*	this study
yBC11H2	S288c *MAT***a** *his3Δ*1 *leu2Δ*0 *ura3Δ*0 *met15Δ*0 *flo11Δ*::GFP-*URA3 tec1Δ*::KanMX4 *FLO8*	this study
yBC16A3	S288c *MAT***a** *ura3Δ*0 *FLO8*	this study
yBC16F4	S288c *MAT***a** */α ura3Δ*0/*ura3Δ*0 *FLO8*/*FLO8*	this study
yBC20A1	S288c *MAT***a** *ura3Δ*0 *tec1Δ*::hyg *FLO8*	this study
yBC20D1	S288c *MATα ura3Δ*0 *tec1Δ*::hyg *FLO8*	this study
yBC20A3	S288c *MAT***a** */α ura3Δ*0/*ura3Δ*0 *tec1Δ*::hyg/*tec1Δ*hyg *FLO8*/*FLO8*	this study
yBC11E8	S288c *MAT***a** *his3Δ*1 *leu2Δ*0 *ura3Δ*0 *met15Δ*0 *flo11Δ*::*HIS3*PEST *FLO8*	this study
yBC11H8	S288c *MAT***a** *his3Δ*1 *leu2Δ*0 *ura3Δ*0 *met15Δ*0 *flo11Δ*::*HIS3*PEST *tec1Δ*::KanMX4 *FLO8*	this study
yBC18A1	S288c *MAT***a** *ura3Δ*0 *rpi1Δ*::*URA3 FLO8*	this study
yBC18A6	S288c *MAT***a** *ura3Δ*0 *rpi1Δ*::*RPI1*^{Sigma} *FLO8*	this study
yBC18A8	S288c *MAT***a** *ura3Δ*0 *rpi1Δ*::*RPI1*^{Sigma} tecΔ1::KanMX4 *FLO8*	this study
yBC29A9	S288c *MAT*a *ura3Δ*0 *RPI1*-3xFLAG-*URA3 FLO8*	this study
yBC29D9	S288c *MAT***a** *ura3Δ*0 *rpi1Δ*::*RPI1*^{Sigma}-3xFLAG-*URA3 FLO8*	this study
10560-6B	Sigma *MATα his3*::hisG *leu2*::hisG *trp1*::hisG *ura3*-52	Fink Collection
yBC0172	Sigma *MAT***a** *his3*::hisG *leu2*::hisG *trp1*::hisG *ura3*-52	this study
Sigma *tec1Δ*	*MAT***a** *can1Δ*::*STE2pr-Sphis5 lyp1Δ*::*STE3pr-LEU2 his3*::hisG *leu2Δ ura3Δ tec1Δ*::KanMX4	Dowell and Ryan et al. (2010)
Sigma *ste7Δ*	*MAT***a** *can1Δ*::*STE2pr-Sphis5 lyp1Δ*::*STE3pr-LEU2 his3*::hisG *leu2Δ ura3Δ ste7Δ*::KanMX4	Dowell and Ryan et al. (2010)
Sigma *ste11Δ*	*MAT***a** *can1Δ*::*STE2pr-Sphis5 lyp1Δ*::*STE3pr-LEU2 his3*::hisG *leu2Δ ura3Δ ste11Δ*::KanMX4	Dowell and Ryan et al. (2010)
Sigma *kss1Δ*	*MAT***a** *can1Δ*::*STE2pr-Sphis5 lyp1Δ*::*STE3pr-LEU2 his3*::hisG *leu2Δ ura3Δ kss1Δ*::KanMX4	Dowell and Ryan et al. (2010)

Sigma *ste12Δ*	*MAT***a** *can1Δ*::*STE2pr-Sphis5 lyp1Δ*::*STE3pr-LEU2 his3*::hisG *leu2Δ ura3Δ ste12Δ*::KanMX4	Dowell and Ryan et al. (2010)
yBC0193	Sigma *MAT***a** *his3*::hisG *leu2*::hisG *trp1*::hisG *ura3*-52 *flo11*pr^{Sigma}*Δ*::*FLO11*pr^{S288c}	this study
yBC0196	Sigma *MAT***a** *his3*::hisG *leu2*::hisG *trp1*::hisG *ura3*-52 *flo11*pr^{Sigma}*Δ*::*FLO11*pr^{S288c} *tec1Δ*::KanMX4	this study
yBC11G1	Sigma *MAT***a** *his3*::hisG *leu2*::hisG *trp1*::hisG *ura3*-52 *flo11Δ*::GFP-*URA3*	this study
yBC11B2	Sigma *MAT***a** *his3*::hisG *leu2*::hisG *trp1*::hisG *ura3*-52 *flo11Δ*::GFP-*URA3* *tec1Δ*::KanMX4	this study
yBC16H3	Sigma *MAT***a** *ura3*-52	this study
yBC16B4	Sigma *MAT*α *ura3*-52	this study
yBC16G4	Sigma *MAT***a** */α ura3*-52/*ura3*-52	this study
yBC20G1	Sigma *MAT***a** *ura3*-52 *tec1Δ*::hyg	this study
yBC20B2	Sigma *MATα ura3*-52 *tec1Δ*::hyg	this study
yBC20C3	Sigma *MAT***a** */α ura3*-52/*ura3*-52 *tec1Δ*::hyg/*tec1Δ*hyg *FLO8*/*FLO8*	this study
yBC11A7	Sigma *MAT***a** *his3*::hisG *leu2*::hisG *trp1*::hisG *ura3*-52 *flo11Δ*::*HIS3*-PEST	this study
yBC11D7	Sigma *MAT***a** *his3*::hisG *leu2*::hisG *trp1*::hisG *ura3*-52 *flo11Δ*::*HIS3*-PEST *tec1Δ*::KanMX4	this study
yBC18G1	Sigma *MAT***a** *ura3*-52 *rpi1Δ*::*URA3*	this study
yBC18G6	Sigma *MAT***a** *ura3*-52 *rpi1Δ*::*RPI1*^{S288c}	this study
yBC18G8	Sigma *MAT***a** *ura3*-52 *rpi1Δ*::*RPI1*^{Sigma} *tecΔ*1::KanMX4	this study
yBC29G9	Sigma *MAT***a** *ura3*-52 *RPI1*-3xFLAG-*URA3*	this study
yBC29B10	Sigma *MAT***a** *ura3*-52 *rpi1Δ*::*RPI1*^{Sigma}-3xFLAG-*URA3*	this study
yBC09H1	S288c^{FLO8}/Sigma *MAT***a** */α ura3Δ*0/*ura3*-52 *his3Δ*0/*his3*::hisG *leu2Δ*0/*leu2*::hisG *met15Δ*0/*MET15 TRP1/trp1*::hisG *tec1Δ*::hyg/*tec1Δ*::hyg *flo11Δ*::GFP-*URA3*/*flo11Δ*::GFP-*URA3*	this study
yBC03A10	S288c^{FLO8}/Sigma *MAT***a** */α ura3Δ*0/*ura3*-52 *his3Δ*0/*his3*::hisG *met15Δ*0/*MET15 tec1Δ*::KanMX4/*tec1Δ*::KanMX	this study

Table S6 List of oligonucleotides used in this study

Name	Sequence (5' to 3')	Description
BCP10	agtgcttaaccggaacaaacc	*FLO8F*
BCP15	tatgatcatgatttacgatgaccgt	*FLO8R*
BCP46	ggaaacaagctgagctggac	Flanking *TEC1*
BCP47	tcgtggtttcatccaagtga	Flanking *TEC1*
BCP191	cccaagcgagacctagagtg	Flanking *STE12*
BCP192	gaacatcgatgccttcacct	Flanking *STE12*
BCP195	aagtgattcgtggggtaacg	Flanking *STE7*
BCP196	tgggttattaatcgccttcg	Flanking *STE7*
BCP199	attctcgcccaacttttcct	Flanking *STE11*
BCP200	tcttcgtgcttccatctgtg	Flanking *STE11*
BCP236	tccccttggtgaaagaaatg	Flanking *kss1*
BCP237	ttgattacagtcgcgtcagc	Flanking *kss1*
BCP249	GGTTCTAATTAAAATATACTTTTGTAGGCCTCAAAAATCCATATACGCACACTatgacagagcagaaagccctag	to replace the *FLO11* ORF with *HIS3*
BCP257	tgatgagggtgaagggaaac	*RPI1* swap
BCP316	ggtGCATCCAACTTGAACATTTCGAGAAAGC	For amplifying PEST seq from *CLN2*
BCP317	CTATATTACTTGGGTATTGCCCATACC	For amplifying PEST seq from *CLN2*
BCP320	GCTTTCTCGAAATGTTCAAGTTGGATGCacccataagaacacctttggtggag	linearize pRS313 to add PEST seq from *CLN2*
BCP321	GGTATGGGCAATACCCAAGTAATATAGtgacaccgattatttaaagctg	linearize pRS313 to add PEST seq from *CLN2*
BCP324	atttaagaatgaaaacatcgtaatgaagaaacgaacatgttggaattgtatcaCTATATTACTTGGGTATTGCCCATACC	To replace *FLO11* with *HIS3PEST*
BCP358	CTTTTTTTTAAGTCTTTTTTTTTTTTTTCTCATCATTTTATTACTGATATTTATAAAagattgtactgagagtgcac	*rpi1::ura3*
BCP359	TAGAATTAAAGGGGTAGAAAATTTATGGTGGAGACTTCCCGATACATACTctgtgcggtatttcacaccg	*rpi1::ura3*
BCP360	cgtattcgtttaactatttctcagtcc	*RPI1* swap
BCP412	ctcaacagcagatccagcag	*MSS11F* repeats
BCP413	gaaggcataagtccggttga	*MSS11R* repeats
BCP419	cattgaagccgaacaagaatg	*RPI1F* repeats
BCP420	cttgactgaatatgctctggtg	*RPI1R* repeats
BCP423	tgcaagatttcaggctgttt	*SLT2F* repeats
BCP424	atccacatctgaaggctgct	*SLT2R* repeats
BCP534	GACTACAAGGATGATGACGATAAAGGTGACTATAAAGATCATGACATTGATTATAAAGACCATGACTAAgcaggtcgacaacccttaat	to build a C terminal flag tagging construct
BCP535	GCGGCCGCATAGGCCACT	to build a C terminal flag tagging construct
BCP536	ACCGTTGCATAATATGTCAACTTCAGACTCAGAAAATTTTATGCAACAACATgactacaaggatgatgacgata	C-terminally tag *RPI1* with FLAG
BCP537	GAATTAAAGGGGTAGAAAATTTATGGTGGAGACTTCCCGATACATACTTTAgcggccgcataggccact	C-terminally tag *RPI1* with FLAG
BCP572	cattaaacccgtggaacagc	*GAL11F* repeats
BCP573	gggaataggtgccactttca	*GAL11R* repeats

BCP574	ctgaatgggtggatccaaat	*URA2F* repeats
BCP575	agaacagatggatcacctgga	*URA2R* repeats
BCP576	gaaccggcaagacttaacca	*EPL1F* repeats
BCP577	ttctgtttcgcttctgaattg	*EPL1R* repeats
BCP580	ggacaggagcaggaagaaaa	*NUP159F* repeats
BCP581	tccgaatgcagatgtaccaa	*NUP159R* repeats
BCP584	atgggcataaacggtgacat	*VHS3F* repeats
BCP585	agatcgctgtagccctcctt	*VHS3R* repeats
BCP586	aacctgcacaggaaacatcc	*TFA1F* repeats
BCP587	ctgaagcagtggcagtagca	*TFA1R* repeats
BCP588	cccacgactacaagcacaaa	*WSC4F* repeats
BCP589	cttgtagaaatgggggctga	*WSC4R* repeats
BCP628	aaggctgcagtggtcaagtt	*DNF2F* repeats
BCP629	atatctgaactgcccgatgg	*DNF2R* repeats
BCP632	tacaatcccacgcagtttca	*ULP2F* repeats
BCP633	ttccgtagttgcatcatcaaa	*ULP2R* repeats
BCP634	gctggaaaacgactcaaagc	*SPT8F* repeats
BCP635	agcagccttttgctcatcat	*SPT8R* repeats
BCP636	atgatgagcaaaaggctgct	*SPT8F* repeats
BCP637	tccattagcagaggcttcgt	*SPT8R* repeats
BCP638	ctgtgtcaggacgccataga	*RIM15F* repeats
BCP639	tccttggggaaaactgaaaa	*RIM15R* repeats
BCP640	tcaaatgtgatgccaggttc	*SNF2F* repeats
BCP641	ttgctcggcagtaaacattg	*SNF2R* repeats
BCP642	agtacggggaccttgaacct	*SWE1F* repeats
BCP643	tacgagaatccacgctttcc	*SWE1R* repeats
BCP644	cagctggtgttcagggaaat	*PTP3F* repeats
BCP645	ccaaatcaggccaatttttc	*PTP3R* repeats
BCP646	acaacggcgatgaaaagaat	*MED2F* repeats
BCP647	tgccgttatcgtcattgttg	*MED2R* repeats
BCP648	aggctggataacctgcaaga	*DSN1F* repeats
BCP649	ttgcagtcgcatctccacta	*DSN1R* repeats
BCP650	caagaccattcgctgcagta	*IXR1F* repeats
BCP651	taaggcgcttgttgttgttg	*IXR1R* repeats
BCP654	atgggaactccaaccgtaca	*PGD1F* repeats
BCP655	agtcgactgctgtgcgtaga	*PGD1R* repeats
BCP656	ccaataacaccccgctacag	*PGD1F* repeats
BCP657	tactgtggttgaggctgctg	*PGD1R* repeats
BCP658	tagtttgaaggaacgcgaca	*UBP10F* repeats
BCP659	gaacccaagttttcaccaatg	*UBP10R* repeats
BCP660	atgattcagcaacgacacca	*SNF5F* repeats

BCP661	aggaggaggggtagaagtcg	*SNF5R* repeats
BCP662	tgttgcacaacaacaagtgc	*SNF5F* repeats
BCP663	gctgttgtcgctgtatttgg	*SNF5R* repeats
FLO11 FW	cacttttgaagtttatgccacacaag	*FLO11* qPCR
FLO11 RV	cttgcatattgagcggcactac	*FLO11* qPCR
ACTI FW	ctccaccactgctgaaagagaa	*ACT1* qPCR
ACTI RV	ccaaggcgacgtaacatagtttt	*ACT1* qPCR